



# Naringenin alleviates hyperglycemia-induced renal toxicity by regulating activating transcription factor 4–C/EBP homologous protein mediated apoptosis

Mohammad Fareed Khan<sup>1,2</sup> · Alpana Mathur<sup>1</sup> · Vivek Kumar Pandey<sup>1,2,3</sup> · Poonam Kakkar<sup>1,2</sup>

Received: 10 April 2021 / Accepted: 1 September 2021 / Published online: 6 October 2021  
© The International CCN Society 2021

## Abstract

Endoplasmic reticulum (ER) dysfunction plays a prominent role in the pathophysiology of diabetic nephropathy (DN). This study aimed to investigate the novel role of Naringenin (a flavanone mainly found in citrus fruits) in modulating ER stress in hyperglycemic NRK 52E cells and STZ/nicotinamide induced diabetes in Wistar rats. The results demonstrated that Naringenin supplementation downregulated the expression of ER stress marker proteins, including p-PERK, p-eIF2 $\alpha$ , XBP1s, ATF4 and CHOP during hyperglycemic renal toxicity in vitro and in vivo. Naringenin abrogated hyperglycemia-induced ultrastructural changes in ER, evidencing its anti-ER stress effects. Interestingly, treatment of Naringenin prevented nuclear translocation of ATF4 and CHOP in hyperglycemic renal cells and diabetic kidneys. Naringenin prevented apoptosis in hyperglycemic renal cells and diabetic kidney tissues by downregulating expression of apoptotic marker proteins. Further, photomicrographs of TEM confirmed anti-apoptotic potential of Naringenin as it prevented membrane blebbing and formation of apoptotic bodies in hyperglycemic renal cells. Naringenin improved glucose tolerance, restored serum insulin level and reduced serum glucose level in diabetic rats evidencing its anti-hyperglycemic effects. Histopathological examination of kidney tissues also confirmed prevention of damage after 28 days of Naringenin treatment in diabetic rats. Additionally, Naringenin diminished oxidative stress and improved antioxidant defense response during hyperglycemic renal toxicity. Taken together, our study revealed a novel role of Naringenin in ameliorating ER stress during hyperglycemic renal toxicity along with prevention of apoptosis, cellular and tissue damage. The findings suggest that prevention of ER stress can be exploited as a novel approach for the management of hyperglycemic nephrotoxicity.

**Keywords** ER Stress · Diabetic Nephropathy · Naringenin · Oxidative Stress · Apoptosis · Unfolded protein response

## Abbreviations

|     |                           |
|-----|---------------------------|
| DN  | Diabetic Nephropathy      |
| UPR | Unfolded Protein Response |
| HG  | Hyperglycemia             |
| NR  | Naringenin                |
| ER  | Endoplasmic Reticulum     |

|               |  |
|---------------|--|
| PERK          | Protein kinase RNA like endoplasmic reticulum kinase |
| eIF2 $\alpha$ | Eukaryotic translation initiation factor 2 $\alpha$  |
| XBP1s         | X-box binding protein 1-spliced                      |
| ATF4          | Activating Transcription Factor 4                    |
| CHOP          | C/EBP Homologous Protein                             |
| Bax           | Bcl2 Associated Protein X                            |
| Bcl2          | B-cell Lymphoma 2,                                   |
| Caspase 3     | Cysteine Aspartic Acid Protease 3                    |
| T2D           | Type2 Diabetes                                       |
| STZ           | Streptozotocin                                       |
| OGTT          | Oral Glucose Tolerance Test                          |
| NRK 52E       | Normal Rat Kidney 52E                                |
| IRE1 $\alpha$ | Inositol Requiring Enzyme 1                          |
| ATF6          | Activating Transcription Factor 6                    |
| JNK           | C-Jun N-Terminal Inhibitory Kinase                   |
| TRAF2         | Tumor Necrosis Factor Receptor Associated Factor 2   |

✉ Poonam Kakkar  
kakkarp59@gmail.com

<sup>1</sup> Herbal Research Laboratory, CSIR-Indian Institute of Toxicology Research (CSIR-IITR), Vishvighyan Bhavan, 31, Mahatma Gandhi Marg, Lucknow, Uttar Pradesh 226001, India

<sup>2</sup> Academy of Scientific and Innovative Research (AcSIR), Ghaziabad 201002, India

<sup>3</sup> Department of Pharmacology and Nutritional Sciences, College of Medicine, University of Kentucky, Lexington, USA

|       |                                   |
|-------|-----------------------------------|
| BiP   | Binding immunoglobulin Protein    |
| TM    | Tunicamycin                       |
| ROS   | Reactive Oxygen Species           |
| ELISA | Enzyme-Linked Immunosorbent Assay |
| GSH   | Reduced glutathione               |
| SOD   | Superoxide Dismutase              |
| TUDCA | Tauroursodeoxycholic Acid         |
| TEM   | Transmission Electron Microscopy  |

## Introduction

Diabetic nephropathy (DN) is one of the severe outcomes of diabetes and is commonly associated with mortality in diabetic patients worldwide (Sulaiman 2019). However, molecular mechanisms underlying the pathogenesis of the disease are poorly explored. Several factors like oxidative stress, inflammation, mitochondrial dysregulation along with endoplasmic reticulum (ER) stress are reported to be involved in the pathophysiology of DN (Gurley et al. 2018; Mathur et al. 2018; Saxena et al. 2019; Mo et al. 2019). Redox homeostasis in the ER is crucial for the maturation and proper folding of proteins. Hyperglycemia induces overproduction of free radicals which disrupt the redox environment culminating in oxidative misfolding of proteins and their subsequent accumulation in the ER lumen. ER being metabolically active, plays a major role in the homeostasis of proteins, including translation, maturation, folding, secretion and degradation of secretory and membrane proteins (Acosta-Alvear et al. 2018). Several pathophysiological conditions, including hyperglycemia owing to the abnormal accumulation of unfolded or improperly folded proteins in ER, result in the induction of the unfolded protein response (UPR) pathways (Pandey et al. 2019; Almanza et al. 2019). Various reports suggest that aberrant activation of UPR sensors exacerbates diabetic complications (Ju et al. 2019).

UPR pathway is a self-protective mechanism that enhances the protein folding capacity and removes defective proteins. However, if the stress is prolonged, apoptotic signaling is induced, which proves fatal for the cells (Ghemrawi et al. 2018). UPR comprises of three trans-membrane sensors namely inositol requiring enzyme 1 (IRE1 $\alpha$ ), protein kinase RNA-like ER kinase (PERK) and activating transcription factor 6 (ATF6). These UPR sensors remain inactive due to blocking of their luminal domains by ER-resident chaperone i.e. Binding immunoglobulin Protein (BiP) under normal conditions (Van et al., 2019). However, upon accumulation of misfolded proteins, BiP gets dissociated from luminal domains of UPR sensors to assist in the proper folding of misfolded proteins (Pobre et al. 2019). During cellular stresses, ATF6 gets cleaved by site 1 and site 2 specific proteases in the Golgi body and acts as a transcription factor to combat ER stress (Liu and Green 2019).

Active IRE1 $\alpha$  splices the mRNA of X-Box Binding Protein 1 (XBP1) to its active state, i.e. XBP1s which regulates the synthesis of protein folding enzymes and chaperones (Tsuchiya et al. 2018). Activated PERK phosphorylates eukaryotic translation initiation factors 2 $\alpha$  (eIF2 $\alpha$ ) at Ser51 residue and inhibits global protein synthesis to maintain ER proteostasis (Rozpedek et al. 2016). However, a subset of mRNAs is preferentially translated namely activating transcription factor 4 (ATF4) and CCAAT/enhancer-binding protein (C/EBP) homologous protein (CHOP) which inhibit Bcl2 (B-cell lymphoma 2) and activate cell death pathways (Ghemrawi et al. 2018). Hyperglycemia-induced ER stress mediated apoptosis of kidney cells leads to impaired renal functions, which further aggravate DN (Liu et al. 2008). In the last few years, many studies have reported the key role of ER stress and associated molecular mechanisms involved in hyperglycemic renal toxicity. However, proper management of the disease is still lacking due to poorly explored mechanisms and lack of effective treatments compelling for further investigations to understand the disease pathology. Activation of the PERK-eIF2 $\alpha$  pathway is reported to be the major contributor to the pathogenesis of DN (Ju et al. 2019). Exploration of ER stress inhibition is a promising approach in the management of diabetic renal toxicity (Sun et al. 2016; Mo et al. 2019).

Naringenin, a flavanone is mainly found in citrus fruits such as grapefruits and oranges (Zobeiri et al. 2018). Naringenin is reported to show a wide array of biological effects such as anti-hyperglycemic, antioxidant and anti-inflammatory activities (Kapoor and Kakkar 2014). Earlier reports have shown the protective effects of Naringenin in various diseases, including diabetic hepatopathy, cardiovascular disease and renal dysfunction (Kapoor and Kakkar 2014; Tang et al. 2017). However, it is still not reported whether Naringenin has protective effects against ER stress during hyperglycemic renal toxicity. In the present study, we demonstrate for the first time that Naringenin has protective effects against hyperglycemia-induced ER stress in vitro and in vivo.

## Materials and methods

### Reagents and antibodies

Antibodies including  $\beta$ -Actin (sc-47778), PERK (sc-23073), eIF2 $\alpha$  (sc-11386), Caspase-3 (sc-7148), Bax (sc-493), Bcl2 (sc-492), Protein A/G PLUS Sepharose beads (sc-2003) and anti-rabbit FITC (sc-2012) were obtained from Santa Cruz Biotechnology (Santa Cruz, CA, USA). p-PERK (3179), p-eIF2 $\alpha$  (3597), ATF4 (11815), CHOP (2895) and HRP tagged anti-mouse antibodies (7076S) were procured from Cell Signalling Technology (CST, Danvers, MA,

USA). Anti-XBP-1 antibody (ab198999), Alexa Fluor 488 tagged secondary antibody (ab150077) and Hoechst 33,258 (ab228550) were purchased from Abcam, (Cambridge MA, USA). Cyanine3 (Cy3) conjugated secondary antibody was procured from Thermo Fisher Scientific (Carlsbad, CA, USA). Naringenin (N5893), Streptozotocin (S0130), Nicotinamide (N3376), Glucose (G8270), Tunicamycin (T7765), HRP tagged anti-rabbit (A0545) secondary antibody was purchased from Sigma-Aldrich (St. Louis, MO, USA). All the other chemicals and reagents used in the experiments were procured from Sigma-Aldrich (St. Louis, MO, USA) with high purity and analytical grade.

### Cell culture and treatment schedule

Rat renal proximal tubular epithelial cell line (NRK 52E) was procured from American type culture collection (ATCC; Manassas, VA, USA). The cells were cultured in Dulbecco's Modified Eagle's Medium (DMEM-low glucose, Cat. No. D5523, Sigma-Aldrich St. Louis MO, USA) supplemented with 3.7 g/lit sodium bicarbonate, 10% heat-inactivated fetal bovine serum, 1% v/v antibiotic-antimycotic solution (Gibco Life Technologies, Grand Island, NY, USA) at 37 °C in a humidified incubator (Thermo Fisher Scientific, Model-Heracell vios160i) containing 5% atmospheric CO<sub>2</sub> and 95% air. Hyperglycemia was induced in NRK 52E cells by supplementing additional 25 mM glucose (Final concentration 30 mM) while Mannitol (30 mM) was used as an osmotic control for 48 h (Mathur et al. 2018). Tunicamycin (TM) was employed to induce ER stress in renal cells and it served as a positive control. Tunicamycin was dissolved in DMSO to prepare a stock solution of 0.5 mg/mL which was further diluted in culture medium. Tunicamycin was added to the growth medium of the cells to achieve the final concentration of 2 µg/mL of culture medium for 24 h (Mo et al. 2019). Naringenin powder was dissolved in DMSO to form 0.5 M stock solution which was further diluted in culture medium to the appropriate concentrations for in vitro experiments. The final concentration of DMSO was less than 0.1% in the working solution of Naringenin.

### Tetrazolium dye reduction assay

The viability of NRK 52E cells was examined by tetrazolium dye MTT [3-(4, 5-dimethylthiazol-2yl)-2, 5-diphenyltetrazolium bromide] reduction assay (Mosmann 1983). Briefly, 100 µl of cell suspension ( $1 \times 10^4$  cells/well) was added to a 96 well plate and allowed to grow. After 24 h, cells were co-treated with high glucose (30 mM) and different concentrations of Naringenin (10, 15, 25 and 50 µM) for 48 h. After the indicated time, 0.5 mg/mL MTT solution was added per well and incubated in a CO<sub>2</sub> incubator at 37 °C for an additional 4 h. Thereafter, media was discarded and 100µL

DMSO was added to each well and incubated at room temperature for 30 min to dissolve formazan crystals produced by mitochondrial dehydrogenases in metabolically active cells. Absorbance was measured at 570 nm by microplate spectrophotometer (Varioskan Flash, Thermo Fisher Scientific, Waltham, MA, USA). Cell viability was calculated by considering control cells as 100% viable.

### Alamar blue reduction assay

Alamar blue is a cell-permeant dye that indicates cell viability by using their reducing potential. Briefly, cells ( $1 \times 10^4$ /well) were seeded in a black 96 well plate and allowed to adhere for 24 h. Cells were co-treated with high glucose (30 mM) and different doses of Naringenin (10, 15, 25 and 50 µM) for 48 h. After the indicated time, Alamar blue reagent (10 µl/well) was added and incubated for 3 h in a CO<sub>2</sub> incubator. Fluorescence was read at Ex/Em wavelengths of 530/590 nm in a microplate reader (Varioskan Flash, Thermo Fisher Scientific, Waltham, MA, USA). Results are expressed as percentage cell viability compared to untreated cells (Larson et al. 1997).

### Propidium iodide uptake assay

Propidium iodide (PI) is a cell-permeant fluoroprobe that is widely used to assess apoptotic cell death. Cells undergoing apoptosis lose their membrane integrity in which PI gets internalized easily and binds with DNA which gives red fluorescence. Briefly,  $1 \times 10^4$  cells/well were seeded in a black 96 well plate and allowed to attach on the bottom followed by co-treatment with high glucose and various doses of Naringenin for 48 h. After the indicated time, PI (1 mg/mL) was added and incubated for 30 min in a CO<sub>2</sub> incubator. Fluorescence was read at Ex/Em of 535/610 nm on a microplate reader (Varioskan Flash, Thermo Fischer Scientific, Waltham, MA, USA).

### Hoechst staining

Hoechst staining was performed to examine the nuclear condensation, DNA fragmentation and karyopyknosis in control and treated cells. In brief, cells were seeded at a density of  $1.0 \times 10^5$  on glass coverslips into a 6 well plate and allowed to adhere for 24 h. Thereafter, cells were co-treated with high glucose and various doses of Naringenin (10, 15, 25 and 50 µM) for 48 h. After the indicated time of incubation, cells were washed thrice with PBS and fixed with 4% paraformaldehyde for 15 min and again washed with 1X PBS. After that Hoechst 33258 (10 µg/mL) was added for 5 min and washed thrice with PBS and mounted in glycerol. Images were visualized under high resolution

fluorescence microscope (Nikon, Eclipse 80i, Tokyo, Japan) at 20X magnification.

### Estimation of reactive oxygen species (ROS) generation

Intracellular ROS production was measured as per the protocol published earlier (Shukla et al. 2014) using cell-permeant ROS-sensitive fluorescence molecule 2', 7'- dichlorodihydro-fluorecein diacetate (DCFH-DA; Sigma-Aldrich, St. Louis, MO, USA). Briefly, NRK 52E cells ( $1.0 \times 10^4$  cells/well) were seeded in a black 96-well plate and allowed to adhere for 24h. After that, cells were treated with high glucose (30 mM; 48 h) and high glucose + Naringenin (25  $\mu$ M; 48 h). After 24 h, tunicamycin (TM, 2  $\mu$ g/mL; 24 h) was added and incubated for an additional 24 h. After completion of indicated time (48 h), 10  $\mu$ M DCFH-DA (10  $\mu$ l/well) was added and incubated for 30 min in a CO<sub>2</sub> incubator. Fluorescence intensity was measured at Ex/Em wavelength of 485/535 nm by using a fluorescence microplate reader (Varioskan Flash, Thermo Fisher Scientific, Waltham, MA, USA).

### Detection of superoxide generation

The level of superoxide radicals was monitored according to the protocol established in the laboratory (Mathur et al. 2018) using superoxide specific fluorescence indicator dihydroethidium (DHE; Sigma-Aldrich St. Louis MO, USA). DHE gets oxidized to ethidium which intercalates with DNA and gives bright red fluorescence. Briefly, ( $1 \times 10^4$  cells/well) were seeded in a black 96 well plate and allowed to adhere followed by the treatment. After 48 h, DHE (5  $\mu$ g/mL) was added and incubated at 37 °C for 30 min in a CO<sub>2</sub> incubator. Fluorescence intensities of dihydroethidium (Ex/Em-370/420 nm) and ethidium (Ex/Em-535/610 nm) were measured in a fluorescence microplate reader (Varioskan Flash, Thermo Fisher Scientific, Waltham, MA, USA). Index of superoxide generation was calculated by taking the ratio of ethidium/dihydroethidium.

### Assessment of mitochondrial membrane potential

Change in the potential of mitochondrial membranes was examined according to the method of Cossarizza et al. (Cossarizza et al. 1993) and earlier published by our lab (Shukla et al., 2016) using lipophilic fluoroprobe JC1 (Sigma Aldrich, St. Louis MO, USA). In healthy mitochondria, JC1 forms its aggregates (J-aggregates) which emit red fluorescence while in depolarized or unhealthy mitochondria JC1 remains in monomeric form and gives green fluorescence. Briefly,  $1.0 \times 10^4$  cells/well were seeded in a black 96 well plate and incubated for 24 h. After an indicated time,

JC1 dye (5  $\mu$ M) was added to each well and incubated for 30 min at 37 °C in a CO<sub>2</sub> incubator. Fluorescence was read at wavelengths of Ex/Em 535/590 nm (J-aggregates) and Ex/Em 485/535 nm (JC1 monomers). The ratio of red/green fluorescence intensity was used to calculate the change in mitochondrial membrane potential.

### Immunofluorescence staining

Cellular expression of XBP1s and ATF4 and nuclear colocalization of ATF4 and CHOP proteins were determined through immunocytochemistry. In brief, NRK 52E cells ( $1.0 \times 10^5$ ) were grown on glass coverslips in a 6 well plate. After 48 h of treatment, washing of the cells was done thrice with ice-cold 1XPBS, (pH-7.4) followed by fixation with 4% paraformaldehyde (PFA) for 15 min. After fixation, cells were permeabilized with 0.025% Triton X-100 (in 1XPBS) for 10 min followed by blocking of non-cellular proteins with blocking buffer [1% bovine serum albumin (BSA) in 0.1% PBST] for 30 min. Cells were then incubated overnight at 4 °C with primary antibody (1:100, in blocking buffer) followed by 2 h incubation with respective secondary antibody (1:200). After washing with 1X PBS, cells were counterstained with Hoechst 33,258 (1  $\mu$ g/mL) for 1 min to stain nuclei of the cells. Images were visualized under a high resolution fluorescence microscope (Nikon, Eclipse 80i, Tokyo, Japan) and a confocal microscope (Zeiss, LSM880, Germany).

### Protein extraction and immunoblotting

Immunoblotting was performed according to the standard procedure. After an indicated time of treatment, cells were washed with 1XPBS (pH 7.4) and suspended in NP-40 lysis buffer (50 mM HEPES, pH 7.4, 1 mM DTT and 1% NP40) with freshly added protease and phosphatase inhibitor cocktail and kept on ice for 30 min. Cells were scraped, collected, sonicated for 30 s and centrifuged at 16,000  $\times$ g for 15 min at 4 °C. The supernatant was collected and marked as total protein lysate. Protein concentration was estimated by bicinchoninic acid assay (Smith et al. 1985). 6X Laemmli buffer [0.375 M Tris (pH 6.8), 12% SDS, 60% glycerol, 0.6 M DTT and 0.06% bromophenol blue] was added to cell lysates to make it 1X, and boiled at 95 °C for 10 min. An equal amount of protein (30–60  $\mu$ g) was loaded in each well and proteins were resolved on 10% SDS-PAGE. Gel was run nearly for 4 h at 60 V and proteins were electrophoretically transferred to PVDF membranes (Hydrophobic Immobilon-P, Millipore, MA, USA) for 3 h at 150 V on a semi-dry transfer unit (TE 77, PWR, GE Healthcare Biosciences, UK). The membrane was blocked overnight with 1% (w/v) non-fat dry milk powder in 1X TBST [Tris- buffered saline having 0.1% Tween 20 (pH-7.6)] at 4 °C. After blocking, the membrane was



washed thrice with 1X TBST using a rocker and incubated overnight with primary antibodies (1:1000 in 1X TBST) against target proteins at 4 °C followed by corresponding HRP conjugated secondary antibody (1:2000 in 1X TBST) for 2 h. After washing with 1X TBST, blots were developed by using an immobilon western chemiluminescent horseradish peroxidase substrate detection kit (Millipore, MA, USA, Cat. No. WBKLS0500) on Amersham Imager Ai600 (GE Healthcare Ltd. UK). Densitometry of all western blot images was performed by ImageJ 1.44p software (National Institute of Health, Bethesda, MD, USA).

### Transmission electron microscopy

To investigate any ultrastructural changes in the ER, renal tubular cells (NRK 52E) were examined by transmission electron microscopy (TEM). Briefly, control and treated cells were washed with 0.1 M sodium cacodylate buffer followed by fixing in a mixture of 2% paraformaldehyde and 2.5% glutaraldehyde at 4 °C for 2 h. After fixation, washing of cells was done by 0.1 M sodium cacodylate buffer and then post-fixation was carried out by adding 1% osmium tetroxide solution for 3 h. Thenafter, cells were pelleted down followed by dehydration with increasing concentrations of acetone (15, 30, 60, 90 and 100%) and twice with propylene oxide for 10 min. After dehydration, cells were embedded in dodecenyl succinic anhydride (DDSA) and Araldite medium and kept at 65 °C for 48 h to make the blocks (Shukla et al. 2014). Sections of 60–80 nm thickness were then cut using an ultramicrotome (Leica EM UC7, Vienna, Austria) followed by mounting them on copper grids. Finally, dual staining was done with uranyl acetate and lead citrate. Photomicrographs were captured by a transmission electron microscope (TEM; TECNAI G2 spirit, FEI, Netherland).

### In vivo studies

In vivo studies were performed to confirm in vitro findings. Animals were subjected to various treatments as given below for 28 days.

### Animals

Healthy male Wistar rats (6–7 weeks old, 230 ± 10 g) were obtained from the IITR animal house facility and placed in experimental rooms at the temperature of 25 ± 2 °C with 40–70% humidity and alternate light/dark cycle of 12 h. Animals were fed a standard pellet diet (Altromin International, Germany) and water ad libitum. Before conducting animal experiments, all the protocols were approved by the (IAEC), Institutional Animal Ethics Committee with the approval number IITR/IAEC/08/2018. The entire animal study

was conducted according to the internationally approved guidelines.

### Induction of diabetes and treatment

Non-insulin-dependent diabetes mellitus (NIDDM) was induced by the method of Masiello et al. (Masiello et al. 1998). The advantage of using streptozotocin/nicotinamide model of diabetes is the protective effects of nicotinamide in reducing pancreatic beta cells loss so that insulin synthesis and secretion are not inhibited completely which mimics the pathophysiology of type 2 diabetes. This model has been used in several studies to understand the molecular mechanisms of diabetes-associated complications and to assess the anti-diabetic effects of naturally occurring or insulin-mimetic compounds.

Rats were acclimatized for one week. The body weight and blood glucose level of the rats were measured and all rats were found normoglycemic as they had fasting blood glucose levels within the range of 80–120 mg/dL. Rats were randomly divided into five groups. For induction of diabetes, rats were given a single intraperitoneal dose of streptozotocin (STZ; 60 mg/kg bwt) freshly prepared in cold 0.1 M sodium citrate buffer (pH 4.5). 15 min before STZ injection, rats were injected with 120 mg/kg bwt dose of nicotinamide to reduce the cytotoxic effects caused by STZ (Kapoor et al. 2009). After 72 h of STZ injection, blood glucose was measured and rats having blood glucose more than 250 mg/dL were included in the study and served as the diabetic model. Treatment given to rats of different groups was as follows:

*Group I* Control rats received normal saline.

*Group II* Diabetic rats injected with STZ/Nicotinamide to induce stable hyperglycemia.

*Group III* Diabetic rats received Naringenin (25 mg/kg bwt) oral gavage.

*Group IV* Diabetic rats received Naringenin (50 mg/kg bwt) oral gavage.

*Group V* Diabetic rats received Naringenin (100 mg/kg bwt) oral gavage.

The dose of Naringenin was prepared in an aqueous solution of 0.5% sodium carboxymethylcellulose and given once per day by oral gavage. Daily dosing of rats was started after 3 days of STZ injection and completed after 4 weeks. The dose of Naringenin was adjusted according to the changes in the body weight of the animals.

### Oral glucose tolerance test (OGTT)

OGTT was performed to assess the glucose clearance rate in rats according to the standard protocol described by Ghezzi et al. (Ghezzi et al. 2012). Briefly, rats were fasted for 6 h and blood glucose levels were measured. All rats were given glucose solution of (2 g/kg bwt) orally and blood glucose

levels were measured at the time intervals of 0, 30, 60, 90 and 120 min by taking blood samples from the tail vein using a portable glucometer (Accusure, Tai Doc Technology, Taiwan).

### Biochemical analysis of serum

At the completion of four weeks of the experiment, rats were euthanized according to standard procedure. Blood samples were collected from the heart through cardiac puncture and serum was separated for biochemical studies. Quantitative determination of biochemical parameters including serum urea, serum albumin, serum total proteins and serum glucose was performed by an automated biochemical analyzer (Beckman Coulter-AU480, CA, USA).

### Insulin ELISA assay

The level of insulin was measured in the serum samples of rats using insulin ELISA assay kit (Cat. No. PG6642R, Puregene, Genetix Biotech Asia Pvt. Ltd) as per the manufacturer's protocol. The absorbance was read at 450 nm on Varioskan Flash microplate reader (Thermo Fisher Scientific, Waltham, MA, USA). Serum protein levels were estimated by bicinchoninic acid (BCA) assay. Insulin concentration in the serum was calculated using to the standard reference values provided with the kit. Results are expressed as insulin levels of ng/mL blood.

### Histopathological examination of rat kidney

Rats were sacrificed and the kidneys were collected immediately thereafter. Each kidney was dissected and fixed in 10% neutral buffered formalin (10% NBF). Formalin-fixed kidney tissues were embedded in paraffin and cut into 5  $\mu$ m thick sections using a microtome (Leica RM, 2155, Germany) followed by hematoxylin and eosin (H&E) staining to examine the histopathological changes in the kidneys. Images were captured under high resolution microscope (Olympus BX53, Tokyo, Japan) at 40X magnification.

### Co-immunoprecipitation

Interaction of ATF4 and CHOP protein was assessed through co-immunoprecipitation according to the method of Cottrell et al. (Cottrell et al., 2006). In brief, nearly 500  $\mu$ g of nuclear protein sample, freshly isolated from kidney tissues was incubated overnight with anti-ATF4 primary antibody at 4 °C using a tube rotator. After incubation, 20  $\mu$ l of Protein A/G PLUS sepharose beads were added followed by overnight incubation at 4 °C on a tube rotator. Thereafter, washing of the beads was done three times with lysis buffer (NP-40) followed by boiling of the samples in 1X Laemmli

buffer. The samples were then run on 10% SDS-PAGE and their immunoblot analysis was performed according to standard protocol.

### Statistical analysis

Data analysis was performed by using Microsoft Excel 2013 and GraphPad prism software, version 5.01. Results are demonstrated as  $\pm$  SD/SE. Statistical comparison between different groups was calculated by ANNOVA (one-way analysis of variance). The calculated p-values found to be  $<0.05$  between the groups were considered statistically significant.

Details of other methods used in the study are given in the supplementary document.

## Results

### Naringenin prevents cytotoxic effects of high glucose in NRK 52E cells

It has been well established in our lab that high glucose treatment decreases cell viability where 30 mM glucose exposure for 48 h was employed as a standard concentration to induce hyperglycemia in vitro (Mathur et al. 2018). The effect of glucose on the viability of NRK 52E cells was examined by treating them to different concentrations of glucose ranging from 5 to 200 mM for 48 h (Supl. Fig. 1a) Results confirmed that glucose treatment reduced the viability of renal cells in a concentration-dependent manner. At 30 mM glucose concentration, cell viability was significantly reduced to 73.05% ( $p < 0.05$ ) when compared to control as assessed through MTT assay (Supl. Fig. 1a). Therefore, 30 mM glucose was used to induce in vitro hyperglycemic model and selected for further experiments. Earlier studies from our lab demonstrated that Naringenin abrogated oxidative stress and mitochondria-mediated apoptosis by modulating AIF/Endo-G pathway in high glucose cultured primary rat hepatocytes (Kapoor et al. 2013). Therefore, to examine the protective effects of Naringenin on rat renal proximal tubular epithelial cells, we first determined the cytotoxic effects exerted by Naringenin itself by evaluating cell viability of NRK 52E. Hence, cells were exposed to the various concentrations of Naringenin (5–1000  $\mu$ M) for 24, 48 and 72 h to perform MTT assay. Results indicate no significant cell death caused by Naringenin upto 50  $\mu$ M concentration at 24, 48 and 72 h of exposure (Supl. Fig. 1b-d). However, beyond 50  $\mu$ M dose, a significant increase in renal cell death was observed (Supl. Fig. 1b-d). Furthermore, to find out the effective concentration of Naringenin, we selected non-cytotoxic doses of Naringenin (10, 15, 25 and 50  $\mu$ M) based on MTT reduction assay results. NRK

52E cells were co-treated with high glucose (30 mM) and various doses of Naringenin (10, 15, 25 and 50  $\mu\text{M}$ ) for 48 h. Results indicate that 25  $\mu\text{M}$  dose of Naringenin prevented cell death as the viability of NRK 52E cells was increased up to 93.76% ( $p < 0.001$ ) compared to only hyperglycemic renal

cells (Fig. 1A). Alamar blue reduction assay was performed to confirm the protective effects of Naringenin and results showed that 25  $\mu\text{M}$  concentration significantly prevented cell death as the cell viability was significantly increased up to 95.55% ( $p < 0.001$ ) compared to hyperglycemic renal cells

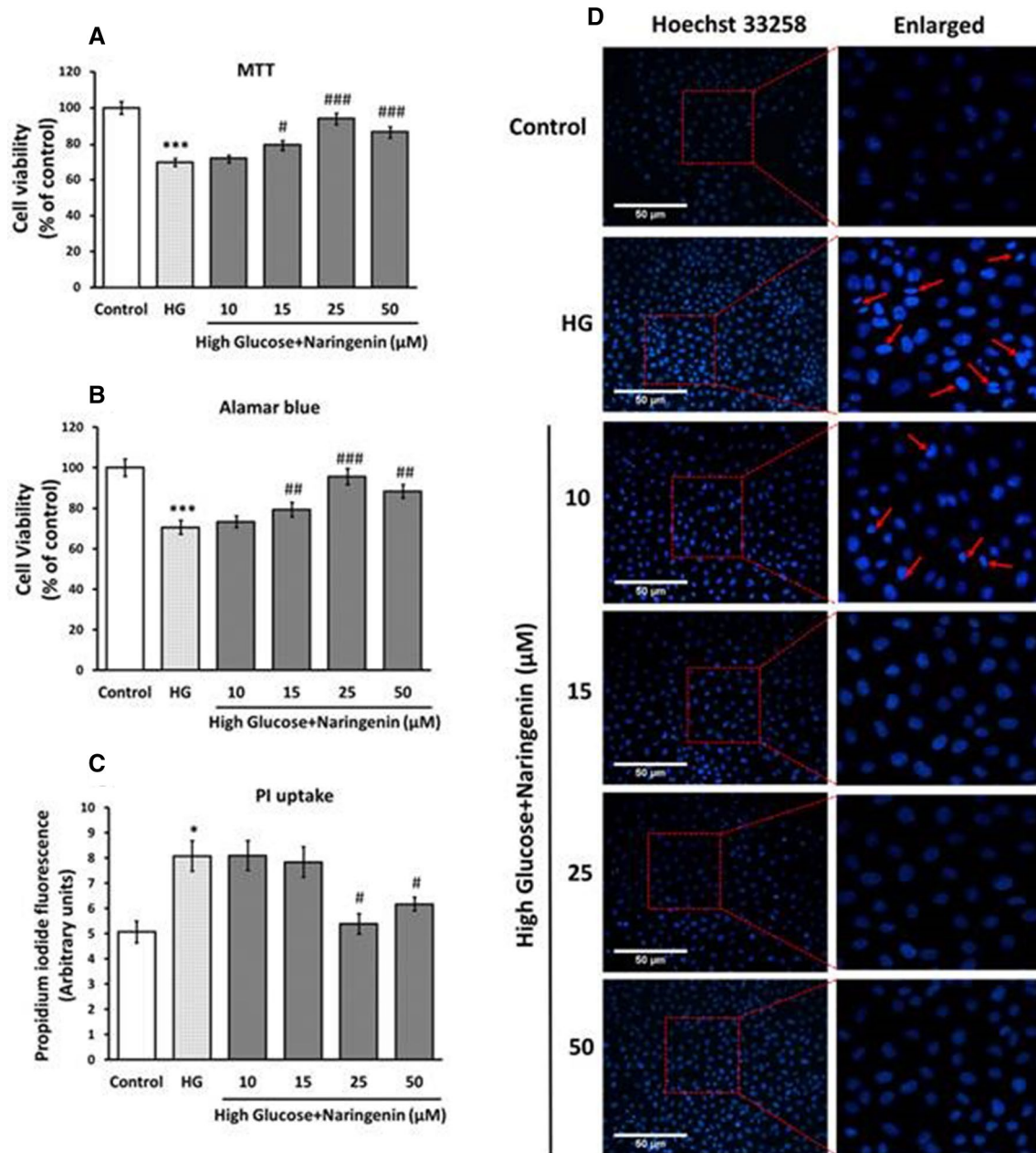


**Fig. 1** Naringenin prevented hyperglycemia induced cytotoxicity in NRK 52E cells. To select the effective concentration of Naringenin, **A** tetrazolium dye (MTT) reduction assay and **B** Alamar blue reduction assays were performed. NRK 52E cells were co-treated with high glucose (30 mM) and several doses of Naringenin (10, 15, 25 and 50  $\mu\text{M}$ ) for 48 h. Bar graphs represent the % viability of NRK 52E cells upon co-treatment of Naringenin at the indicated time. **C** Cell death was evaluated spectrofluorimetrically using propidium

iodide (PI) fluorescent indicator. Bar graph denotes the relative fluorescence intensity of PI upon co-treatment of Naringenin in hyperglycemic renal cells at the indicated time. **D** Fluorescent micrographs of Hoechst 33258 (10  $\mu\text{g}/\text{mL}$ ) stained NRK 52E cells visualized at 20X magnification with scale bar 50  $\mu\text{m}$ . Data are represented as mean  $\pm$  SE. \*  $p < 0.05$ , \*\*\*  $p < 0.001$  indicates significant differences from the control group. #  $p < 0.05$  ##  $p < 0.01$  ###  $p < 0.001$  indicates significant difference from HG group

(Fig. 1B). The results of MTT and Alamar blue reduction assays were further confirmed through propidium iodide (PI) uptake assay, which is an indicator of apoptotic cell death. High glucose treated renal cells displayed a significant increase (1.59 fold,  $p < 0.05$ ) in PI fluorescence intensity compared to untreated cells (Fig. 1C). Conversely, Naringenin treatment at the doses of 25 and 50  $\mu\text{M}$  significantly reduced PI uptake (0.66 fold and 0.76 fold;  $p < 0.05$ ) compared to high glucose exposed NRK 52E cells respectively (Fig. 1C). Furthermore, Hoechst 33,258 staining affirmed the occurrence of apoptotic cell death in hyperglycemic renal cells as evident by nuclear condensation, fragmentation and pyknotic nuclei compared to control (Fig. 1D). Naringenin (25 and 50  $\mu\text{M}$ ) treatment prevented DNA damage and nuclear condensation in high glucose treated renal cells indicating the protective effects of Naringenin during hyperglycemia induced cytotoxicity (Fig. 1D). On the basis of MTT, Alamar blue, PI uptake and Hoechst 33,258 staining results, 25  $\mu\text{M}$  concentration of Naringenin was found most effective than other doses (10, 15 and 50  $\mu\text{M}$ ) therefore, 25  $\mu\text{M}$  dose of Naringenin was selected for further in vitro experiments.

### **Naringenin diminishes oxidative stress and enhances anti-oxidant capacity in hyperglycemic renal cells**

Oxidative stress is a key player in promoting oxidoreductive imbalance in various subcellular compartments, including ER. In the diabetic milieu, enhanced reactive oxygen species (ROS) generation interferes with the protein folding capacity of ER thereby promoting the accumulation of misfolded proteins in ER and cause ER stress (Pandey et al. 2019). Overproduction of ROS has also been linked with activation of ER stress signaling pathway during hyperglycemic nephrotoxicity (Burgos et al., 2019). Therefore, we examined the impact of hyperglycemia on ROS generation and antioxidant defense systems. Further, we checked the ameliorative effects of Naringenin in regulating oxidoreductive imbalance during hyperglycemic nephrotoxicity. Results affirmed that high glucose (30 mM) treated NRK 52E cells demonstrated a noticeable change in intracellular ROS generation as DCF fluorescence intensity was significantly enhanced (1.90 fold,  $p < 0.01$ ) compared to control (Fig. 2A). Overproduction of intracellular ROS was markedly reduced by Naringenin treatment as indicated by reduced DCF fluorescence (0.63 fold,  $p < 0.05$ ) compared to hyperglycemic renal cells (Fig. 2A). In the presence of tunicamycin (an ER stress inducer), renal cells displayed a significant increase in DCF fluorescence intensity (2.11 fold,  $p < 0.01$ ) compared to control, implicating the compromised oxidoreductive balance under ER stress conditions (Fig. 2A). Further, the effect of Naringenin on superoxide radical generation was examined

with DHE dye. A significant increase in the levels of superoxide radicals was evident in the ratio of ethidium/dihydroethidium which was significantly increased in high glucose (1.83 fold,  $p < 0.01$ ) and tunicamycin (2.26 fold,  $p < 0.05$ ) treated renal cells compared to control (Fig. 2B).

Naringenin treatment reduced the generation of superoxide radicals in hyperglycemic NRK 52E cells as indicated by the reduced ratio of ethidium/dihydroethidium (0.57 fold,  $p < 0.01$ ) evidencing its anti-oxidant capacity (Fig. 2B).

Maintaining the membrane potential is crucial for healthy mitochondria whereas stressed or damaged mitochondria exhibit altered membrane potential. The capacity of Naringenin to rescue the mitochondrial membranes from depolarization during hyperglycemic renal toxicity was tested. High glucose treatment in NRK 52E cells altered the membrane potential of mitochondria as evident by the reduced red/green fluorescence ratio (0.43 fold,  $p < 0.01$ ) compared to control indicating towards mitochondrial depolarization (Fig. 2C). Naringenin treatment not only suppressed the intracellular ROS production and superoxide generation but also prevented depolarization of mitochondrial membrane as evident by an increased ratio of red/green fluorescence of JC1 (2.06 fold,  $p < 0.05$ ) under hyperglycemic conditions (Fig. 2C). Treatment of tunicamycin (2  $\mu\text{g}/\text{mL}$ ; 24 h) showed reduced JC1 fluorescence (0.32 fold,  $p < 0.01$ ) compared to control, indicating depolarization and compromised mitochondrial function under ER stress conditions. Further, to examine the anti-oxidant potential of Naringenin, reduced glutathione (GSH) levels as well as antioxidant enzymes such as superoxide dismutase (SOD) and catalase were estimated in control and treated NRK 52E cells. Results demonstrate that treatment of high glucose depleted GSH levels (0.53 fold,  $p < 0.05$ ) compared to control cells, indicating compromised anti-oxidant levels during hyperglycemic renal toxicity (Fig. 2D). Naringenin, on the other hand, guarded renal cells by averting GSH depletion (1.86 fold,  $p < 0.05$ ) hence maintaining the anti-oxidant pool (Fig. 2D). The level of GSH was also checked in presence of ER stress inducer, i.e. tunicamycin. Interestingly, cellular GSH content was significantly depleted (0.58 fold,  $p < 0.05$ ) in tunicamycin treated renal cells compared to control, indicating the inadequacy of reducing equivalents under ER stress conditions (Fig. 2D). Hyperglycemia diminished the activities of antioxidant enzymes, SOD (0.37 fold,  $p < 0.01$ ) and catalase (0.36 fold,  $p < 0.001$ ) compared to control indicating the compromised anti-oxidant defense systems (Fig. 2E-F). However, Naringenin treated hyperglycemic renal cells showed enhanced activities of SOD (2.62 fold,  $p < 0.01$ ) and catalase (1.729 fold,  $p < 0.001$ ) showed the anti-oxidative capacity of Naringenin (Fig. 2E-F). Further, the anti-oxidant enzyme activity of SOD and catalase was monitored in presence of tunicamycin. Data demonstrate a significant depletion in the enzymatic activities of SOD (0.34 fold,  $p < 0.01$ )



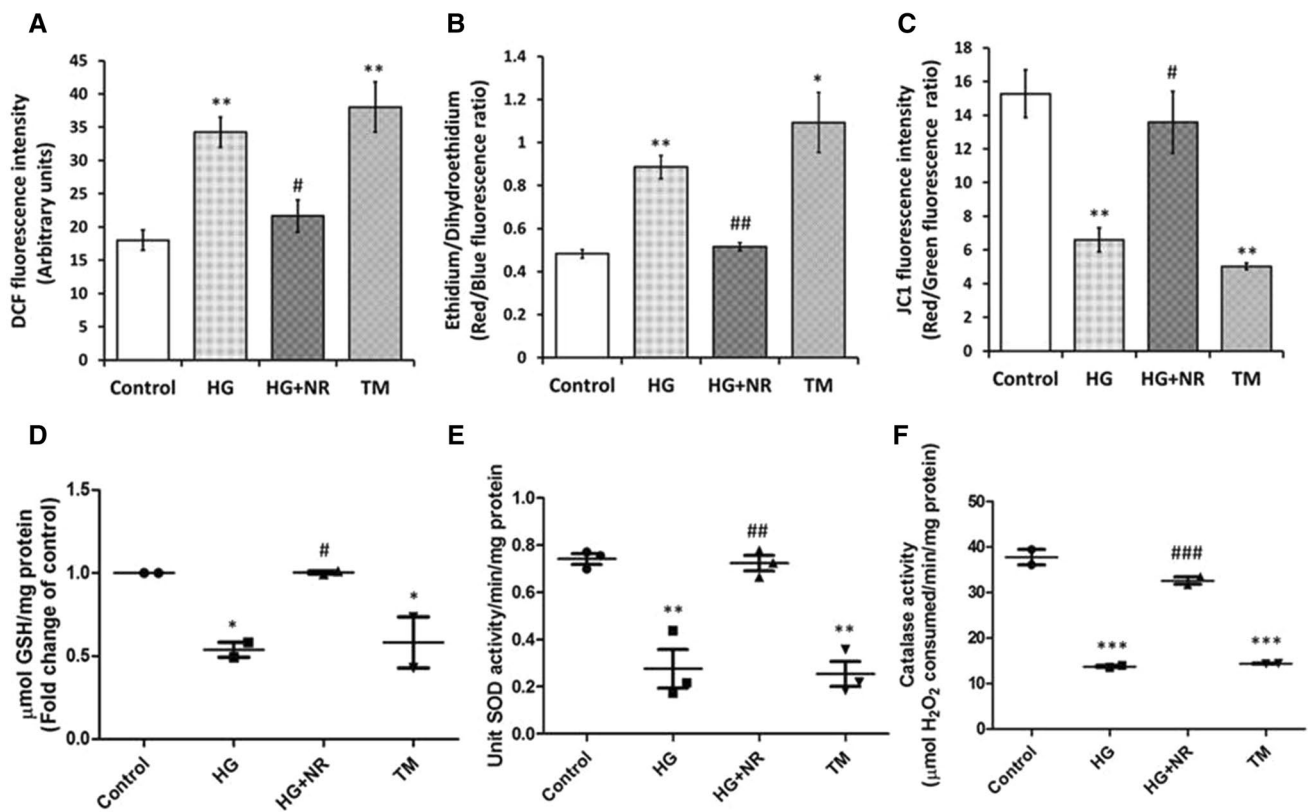


**Fig. 2** Naringenin curbed hyperglycemia-induced oxidative insult in renal cells. **A** NRK 52E cells were co-treated with high glucose (30 mM) and Naringenin (25  $\mu\text{M}$ ) for 48 h. Tunicamycin (TM; 2  $\mu\text{g}/\text{mL}$ ) was used to assess ER stress-induced oxidative stress in renal cells. Total ROS generation was assessed by adding 10  $\mu\text{M}$  DCFH-DA for 30 min and fluorescence was read at Ex/Em of 485/535 nm. The bar graph represents the mean DCF fluorescence intensity expressed in arbitrary units. **B** Superoxide levels were measured by DHE (5  $\mu\text{g}/\text{mL}$ ; 30 min) in NRK 52E cells. The level of superoxide generation was calculated by taking the ratio of ethidium/dihydroethidium. The bar graph represents the fluorescence ratio of ethidium/dihydroethidium. **C** Mitochondrial membrane potential was measured through JC-1 fluoroprobe. The bar graph depicts the ratio of red/green fluorescence intensities. **D** GSH levels were measured in control and treated NRK 52E cells. Dot-plotted graph showing  $\mu\text{mol GSH}/\text{mg protein}$  expressed in fold change of control. **E** Enzymatic activity of SOD was measured in control and treated renal cells. Dot plot graph represents the changes in SOD activity expressed in unit SOD activity/min/mg protein. **F** Dot-plotted graph depicts the catalase activity is presented as  $\mu\text{mol H}_2\text{O}_2$  consumed/min/mg protein. Data are presented as the mean  $\pm$  SE. \*  $p < 0.05$ , \*\*  $p < 0.01$ , \*\*\*  $p < 0.001$  vs control and #  $p < 0.05$ , ##  $p < 0.01$ , ###  $p < 0.001$  vs HG group

and catalase (0.37 fold,  $p < 0.001$ ) compared to control affirming the declined antioxidant enzyme activities under ER stress (Fig. 2E-F). Oxidative damage has been implicated strongly in the promotion and pathogenesis of diabetic kidney disease. So far, the results indicate that Naringenin diminished oxidative stress and improved antioxidant levels in high glucose treated NRK 52E cells. To confirm our in vitro results, the anti-oxidant potential of Naringenin was validated in the renal tissues of STZ/Nicotinamide induced experimental diabetic rats. Data demonstrate increased ROS generation and compromised anti-oxidant defense response as evident through enhanced lipid peroxidation, significant depletion in GSH content and reduced enzymatic activities of SOD and catalase confirming the compromised anti-oxidant response during hyperglycemic nephrotoxicity. (Supl.Fig. 2a-d). On the contrary, Naringenin treatment

proficiently attenuated lipid peroxidation, prevented the loss of GSH content and improved enzymatic activities of SOD and catalase in diabetic kidneys suggesting its anti-oxidant capacity (Supl. Fig. 2a-d). Altogether, results suggest that oxidative insult impaired anti-oxidant machinery during hyperglycemic renal toxicity in vitro and in vivo. However, Naringenin treatment showed protective effects by abolishing oxidative stress and enrichment of anti-oxidant status supporting its renoprotective potency under hyperglycemic conditions.

### Naringenin abrogates hyperglycemia-induced ER stress in vitro and in vivo

ER stress has been reported as a cardinal player in the pathophysiology of DN (Ju et al. 2019). Prolonged exposure to

ER stress inducers such as tunicamycin stimulates cellular damage in renal cells (Mo et al. 2019). To assess the role of Naringenin in regulating hyperglycemia-induced ER stress, we measured the levels of putative ER stress markers including p-PERK, p-eIF2 $\alpha$ , XBP-1 s, ATF4 and CHOP at protein levels. It was observed that high glucose stress in renal cells elevated the phosphorylation of PERK (a major UPR sensor protein), as the expression ratio of p-PERK/PERK was increased significantly (1.65 fold,  $p < 0.001$ ) compared to control indicating the activation of ER stress response during hyperglycemic renal toxicity (Fig. 3A). Activation of PERK signaling axis induces the phosphorylation of its

downstream signaling molecule, i.e. eIF2 $\alpha$  to reduce the protein load in stressed ER. Immunoblot analysis shows increased phosphorylation of eIF2 $\alpha$  as the ratio of p-eIF2 $\alpha$ /eIF2 $\alpha$  was significantly increased (1.54 fold,  $p < 0.01$ ) in high glucose exposed NRK 52E cells compared to control (Fig. 3B). Further, treatment of tunicamycin significantly increased the ratio of p-PERK/PERK (2.18 fold,  $p < 0.001$ ) and p-eIF2 $\alpha$ /eIF2 $\alpha$  (1.49 fold,  $p < 0.01$ ) compared to control indicating the activation of ER stress response in NRK 52E cells (Fig. 3A-B). Importantly, co-treatment of high glucose and Naringenin prevented phosphorylation of PERK and eIF2 $\alpha$  as indicated by the reduced ratio of p-PERK/

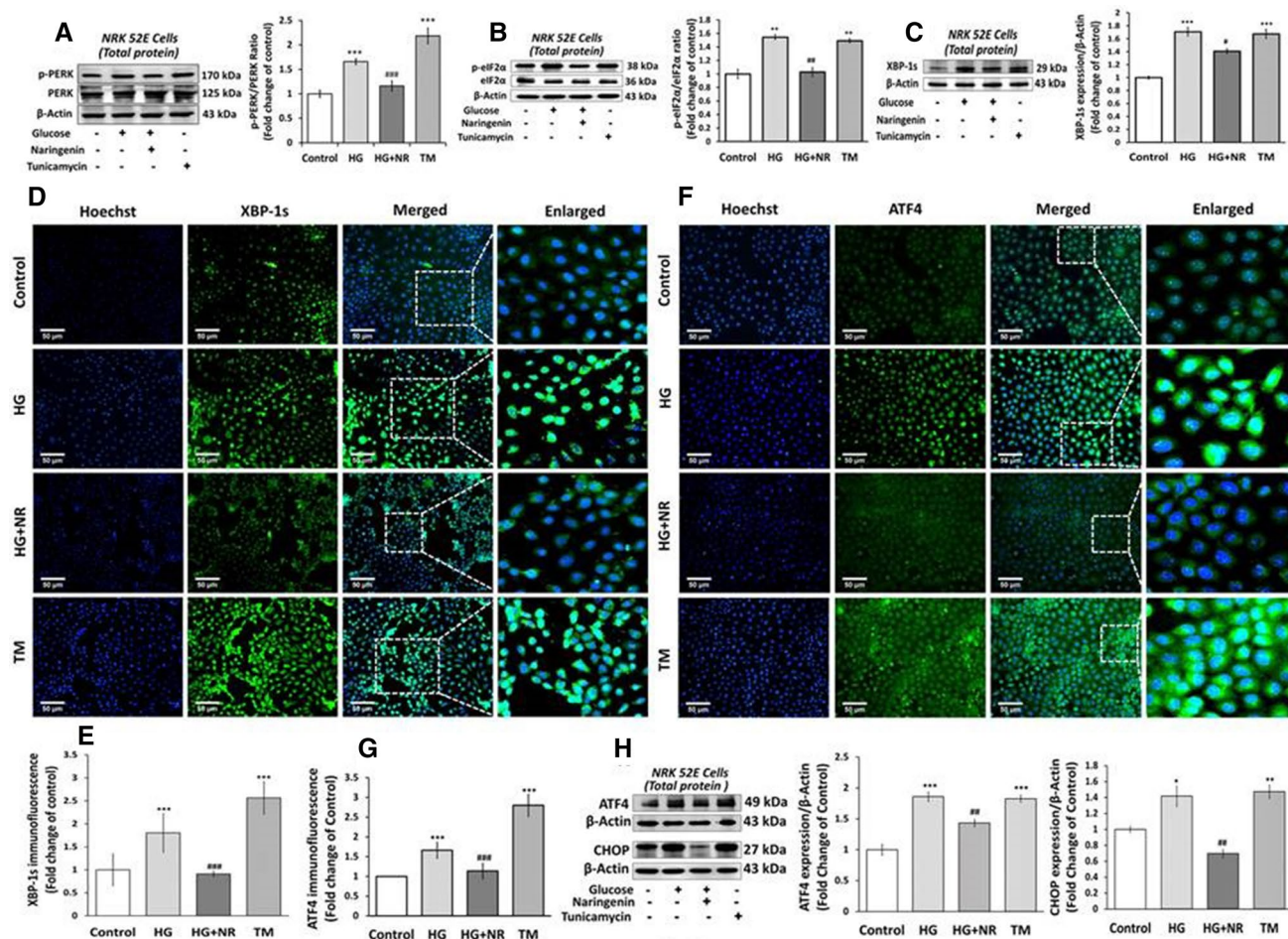


**Fig. 3** Naringenin suppressed hyperglycemia-induced ER stress in vitro. **A** NRK 52E cells were co-treated with high glucose and Naringenin for 48 h. NRK 52E cells were treated with Tunicamycin (TM) at the final concentration of 2  $\mu$ g/mL for 24 h. Total protein lysate was subjected to SDS-PAGE and protein samples were immunoblotted with PERK and p-PERK antibodies. The bar graph shows the densitometric ratio of p-PERK/PERK expressed in the fold change of control. **B** Immunoblots of eIF2 $\alpha$  and p-eIF2 $\alpha$  **C** Immunoblot of XBP1s detected in total protein lysates of control and treated NRK 52E cells. The bar graph shows the densitometric ratio p-eIF2 $\alpha$ /eIF2 $\alpha$  and XBP1s respectively. **D** Fluorescent micrographs showing the cellular expression of XBP1s protein. Cells were visualized under fluo-

rescence microscope at 10X magnification with scale bar 50  $\mu$ m. **E** The bar graph depicts the mean fluorescence intensity expressed in fold change of control. **F** Immunocytochemical staining of ATF4 where Hoechst was used for nuclear stain in blue colour (magnification 20X, scale bar 50  $\mu$ m) in renal cells. **G** Bar graph showing the changes in the level of ATF4 protein. **H** Immunoblots of ATF4 and CHOP were detected in NRK 52E cell lysates. The bar graph shows the densitometry of their respective bands. Band intensities of each blot were normalized to  $\beta$ -actin. Data are presented as the mean  $\pm$  SD/SE. \*  $p < 0.05$ , \*\*  $p < 0.01$ , \*\*\*  $p < 0.001$  vs control and #  $p < 0.05$ , ##  $p < 0.01$ , ###  $p < 0.001$  vs HG

PERK (0.69 fold,  $p < 0.001$ ) and p-eIF2 $\alpha$ /eIF2 $\alpha$  (0.66, fold,  $p < 0.01$ ) compared to hyperglycemic renal cells endorsing the ER stress inhibition capacity of Naringenin (Fig. 3A-B). Further, the protein level of spliced XBP-1 was checked because it is an indicator of ER stress activation. Western blot analysis of XBP-1 s revealed a significant increase (1.7 fold,  $p < 0.001$ ) after 48 h of high glucose treatment compared to untreated cells (Fig. 3C). Upon Naringenin treatment a significant reduction (0.82 fold,  $p < 0.05$ ) in the level of XBP-1 s protein was observed in hyperglycemic renal cells (Fig. 3C) indicating ER stress inhibitory potential of Naringenin. After 24 h exposure of tunicamycin, renal cells showed a substantial increase (1.67 fold,  $p < 0.001$ ) in the expression of XBP-1 s protein compared to control suggesting ER stress activation in renal cells (Fig. 3D-E). Further, XBP-1 s protein expression was confirmed through immunocytochemical studies. A significant increase (1.8 fold,  $p < 0.001$ ) was observed in high glucose treated NRK 52E cells (Fig. 3D-E). On the other hand, Naringenin downregulated XBP-1 s protein expression as indicated by reduced fluorescence (0.50 fold,  $p < 0.001$ ) compared to hyperglycemic NRK 52E cells (Fig. 3D-E) asserting that Naringenin possesses ER stress inhibitory capacity. The deactivation of eIF2 $\alpha$ , a key player of the translational machinery, activates its downstream signaling molecules, including ATF4 and CHOP when the stress is prolonged. Upregulation of ATF4 and CHOP (proteotoxic apoptotic marker proteins) ensures the activation of cell death signals (Ju et al. 2019). NRK 52E cells, exposed to hyperglycemic environment, demonstrated a significant increase in the levels of ATF4 (1.85 fold,  $p < 0.001$ ) and CHOP (1.41 fold,  $p < 0.05$ ) proteins as compared to untreated cells (Fig. 4A). Tunicamycin treated renal cells showed significant upregulation of ATF4 (1.82 fold,  $p < 0.001$ ) and CHOP (1.47 fold,  $p < 0.01$ ) proteins compared to control (Fig. 4A). Interestingly, treatment of Naringenin in hyperglycemic NRK 52E cells downregulated the expression of ATF4 (0.77 fold,  $p < 0.01$ ) and CHOP (0.49 fold,  $p < 0.01$ ) proteins compared to hyperglycemic renal cells showing its anti-ER stress effects (Fig. 3F-H).

To confirm these *in vitro* results, the expression level of molecular markers of ER stress, including p-PERK, p-eIF2 $\alpha$ , ATF4 and CHOP proteins was measured in the kidney tissues of STZ/nicotinamide treated diabetic rats through western blot analysis. Data showed enhanced phosphorylation of PERK and eIF2 $\alpha$  as the ratio of p-PERK/PERK (1.54 fold,  $p < 0.001$ ) and p-eIF2 $\alpha$ /eIF2 $\alpha$  (1.49 fold,  $p < 0.001$ ) were significantly increased in the diabetic kidney tissues as compared to control suggesting the activation of ER stress during DN (Fig. 4A-B). Conversely, supplementation of Naringenin in diabetic rats prevented the activation of the PERK-eIF2 $\alpha$  pathway indicating its ER stress attenuating potential during diabetic renal toxicity (Fig. 4A-B). To further assess the ER stress-induced proteotoxic cell death,

the expression of ATF4 and CHOP proteins was measured in the kidney tissues of control and treated rats. Western blot analysis demonstrates a significant increase in the expression of ATF4 (2.43 fold,  $p < 0.001$ ) and CHOP (1.77 fold,  $p < 0.001$ ) proteins in diabetic kidney tissues compared to control (Fig. 4C-D) indicating ER stress-induced apoptotic cell death. Interestingly Naringenin supplementation (50 mg/kg bwt) for 28 days in diabetic rats significantly downregulated the level of ATF4 (0.69 fold,  $p < 0.001$ ) and CHOP (0.79 fold,  $p < 0.01$ ) protein compared to diabetic rats indicating the protective capacity of Naringenin against ER stress during diabetic renal toxicity (Fig. 4C-D).

### Naringenin prevents nuclear translocation of ATF4 and CHOP during hyperglycemic nephrotoxicity

Activation of proteotoxic apoptotic marker proteins, including ATF4 and CHOP plays an important role in the pathophysiology of many diseases, including diabetes (Oyadomari and Mori 2004). It is reported that ATF4 and CHOP proteins translocate to the nucleus and induce apoptosis under ER stress conditions (Gotoh et al. 2002). Nuclear colocalization of ATF4 and CHOP proteins was examined through immunocytochemistry. Fluorescent micrographs observed under a confocal microscope indicate the nuclear colocalization of ATF4 and CHOP proteins in high glucose, and tunicamycin treated NRK 52E cells compared to control (Fig. 5A). Interestingly, Naringenin treatment prevented the nuclear colocalization of ATF4 and CHOP in hyperglycemic renal cells indicating the critical role of Naringenin in ameliorating ER stress during hyperglycemic nephrotoxicity (Fig. 5A). Further, the level of ATF4 and CHOP proteins was measured in nuclear and cytosolic sub-cellular fractions of kidney tissue lysates. Immunoblot analysis revealed a significant increase in the level of ATF4 (1.88 fold,  $p < 0.001$ ) and CHOP (2.05 fold,  $p < 0.001$ ) proteins in the nuclear fraction of diabetic kidneys compared to control implicating the critical role of ER stress in the progression of DN (Fig. 5B). Conversely, supplementation of Naringenin prevented nuclear translocation of ATF4 and CHOP proteins under diabetic conditions suggesting its ER stress inhibitory effects during hyperglycemic nephrotoxicity (Fig. 5B). To further confirm the protein-protein interaction of ATF4 and CHOP in the nuclear compartment, co-immunoprecipitation was performed. Data suggest that under diabetic conditions, the interaction of ATF4 and CHOP protein was significantly increased (2.27 fold,  $p < 0.001$ ) in the nuclear fraction of diabetic kidney tissue lysate compared to control (Fig. 5D). However, this interaction was significantly lowered in Naringenin (50 and 100 mg/kg bwt) treated diabetic rats affirming its regulatory role on the ATF4-CHOP pathway during hyperglycemic renal toxicity (Fig. 5D). Hence, it can be conceived that Naringenin exerts its protective effects by



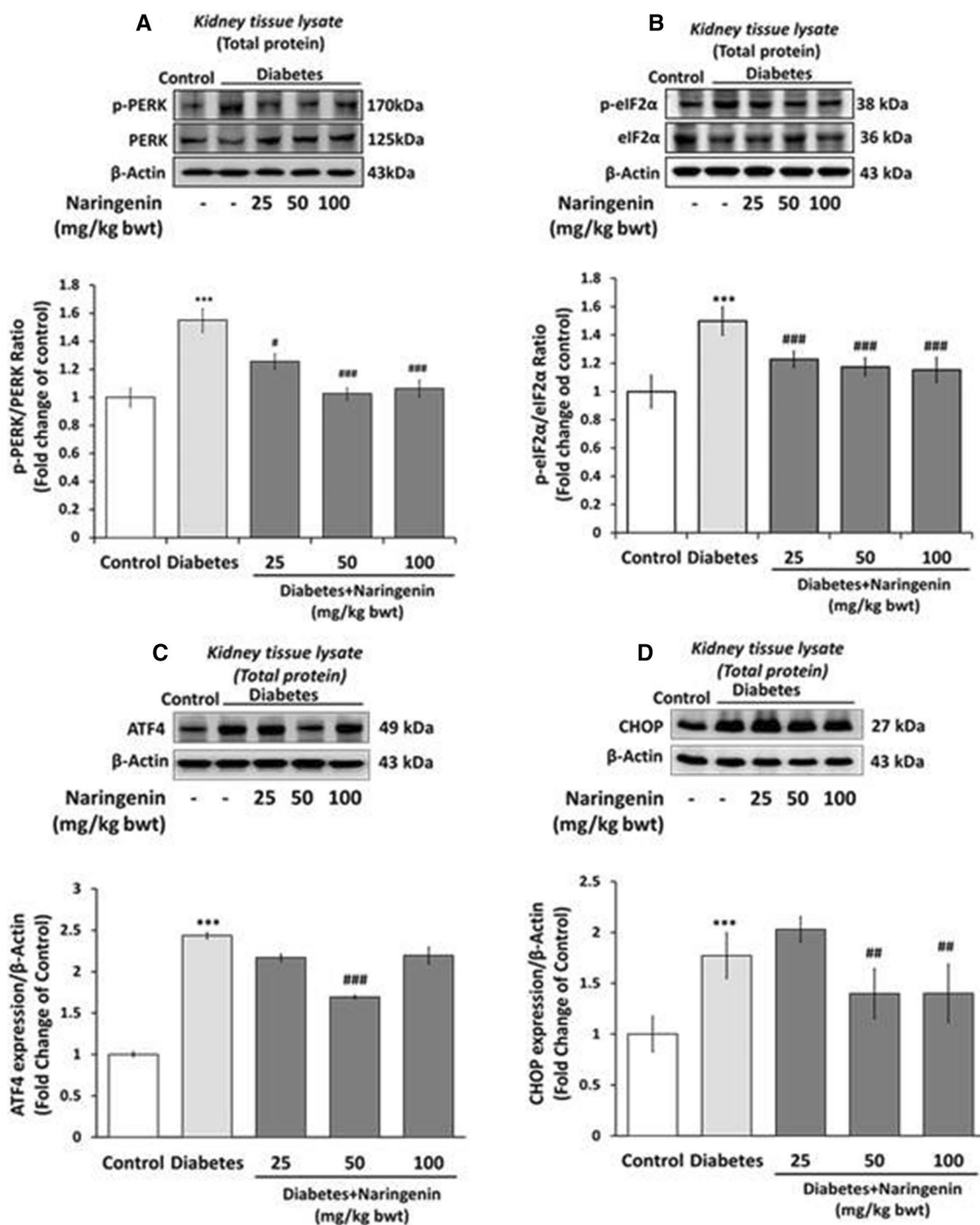


**Fig. 4** Naringenin inhibits ER stress in the kidney tissues of STZ/nicotinamide induced diabetic Wistar rats. Diabetic rats were supplemented with Naringenin for 4 weeks. The expression of ER stress marker proteins was examined in the kidney tissues of control and treated rats through western blotting. Western blots of **A** PERK and p-PERK **B** eIF2 $\alpha$  and p-eIF2 $\alpha$  were detected in total protein lysates.

Bar graphs show the densitometric ratio of p-PERK/PERK and p-eIF2 $\alpha$ /eIF2 $\alpha$  respectively. **C** Immunoblots of ATF4 and **D** CHOP were detected in kidney tissue lysates. The bar graph shows the densitometric analysis expressed as fold change of control.  $\beta$ -actin served as a loading control. Data are presented as mean  $\pm$  SE. \*\*\*  $p < 0.001$  vs control and #  $p < 0.05$ , ##  $p < 0.01$ , ###  $p < 0.001$  vs diabetic rats



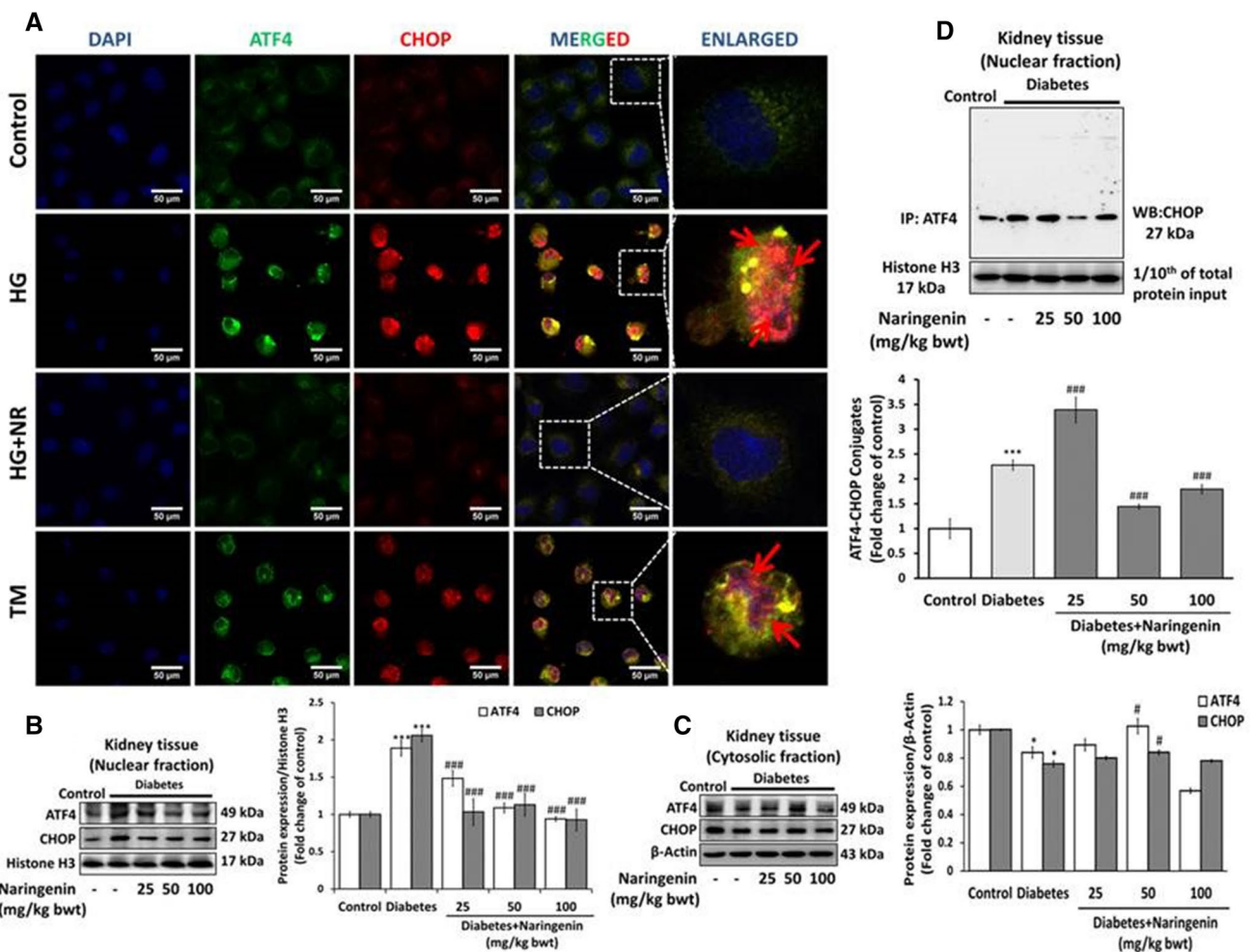


**Fig.5** Naringenin prevents nuclear translocation of ATF4 and CHOP during hyperglycemic nephrotoxicity. **A** Dual immunocytochemical study was performed on control and treated NRK 52E cells to assess the nuclear colocalization of ATF4 and CHOP proteins. ATF4 and CHOP proteins were labeled with Alexa fluor 488 (green) and Cy3 (red) respectively. DAPI (blue) was used to stain the nuclei of the cells. Fluorescent micrographs were captured in a confocal microscope at 40X magnification with scale bar 50 μm. Red arrows indicate the colocalization of ATF4 and CHOP proteins. **B** Immunoblots

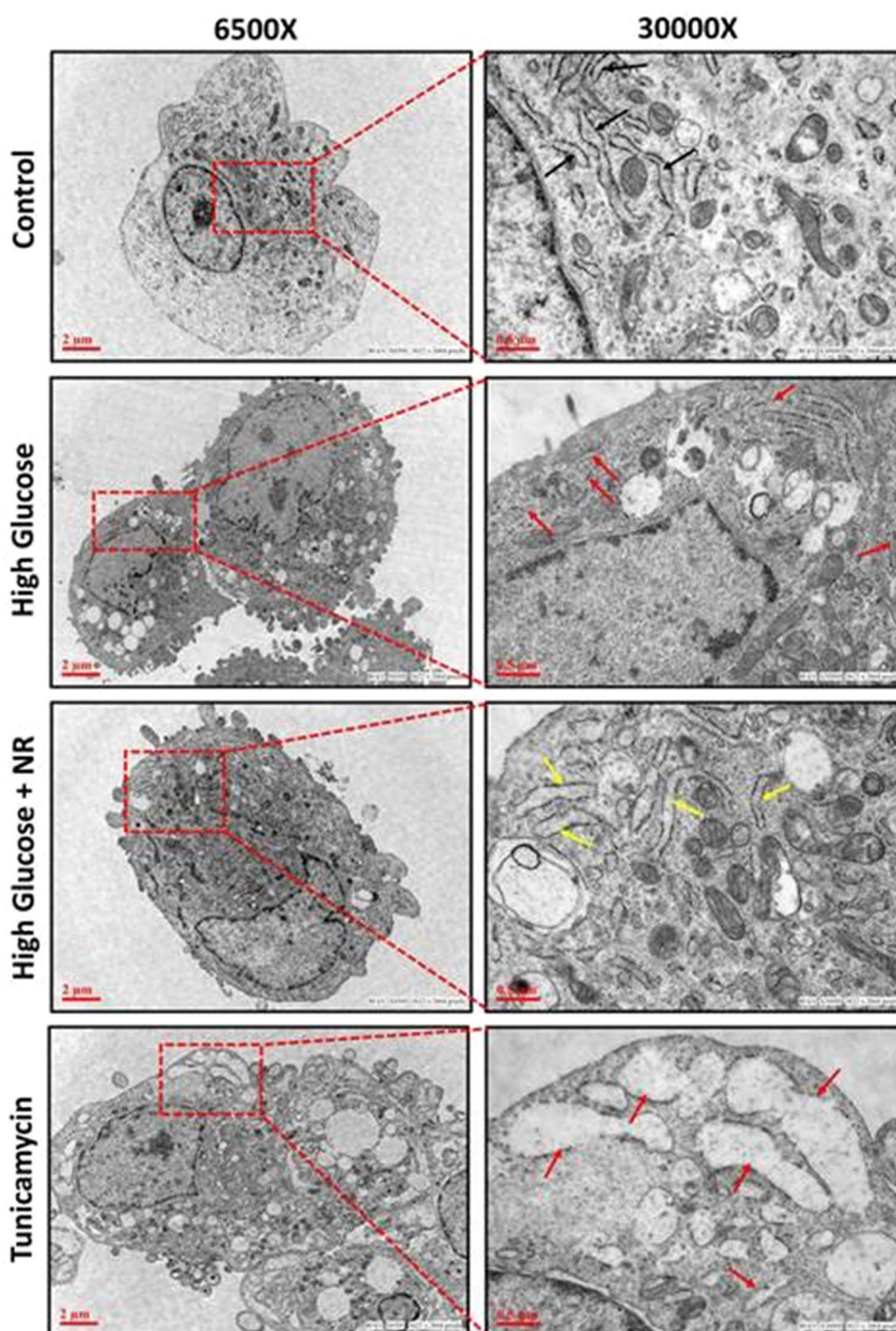
of ATF4 and CHOP measured in nuclear fraction and **C** cytosolic fraction of kidney tissues lysates. Bar graph shows the densitometric analysis expressed as fold change of control. Histone served as an endogenous control for nuclear proteins while β-actin was used as an endogenous control for cytosolic proteins. **D** Western blot of the co-immunoprecipitated nuclear fraction of kidney tissue samples. The bar graph shows the ATF4-CHOP conjugates expressed in fold change of control. Data are presented as mean ± SE. \*  $p < 0.05$ , \*\*\*  $p < 0.001$  vs control and #  $p < 0.05$ , ###  $p < 0.001$  vs diabetes

regulating ATF4-CHOP expression during hyperglycemic nephrotoxicity.

The results so far revealed the protective capacity of Naringenin as it enhanced cell viability, reduced oxidative stress, enhanced anti-oxidant defense and prevented ER stress during hyperglycemic renal toxicity. To further confirm the ER stress inhibitory role of Naringenin, ultrastructural change in the morphology of ER was observed through transmission electron microscopy. Photomicrographs revealed the visible ultrafine changes in the morphology of ER as evident by the disintegration of the ER membrane, dilatation of ER sacs and the loss of native structure of ER in hyperglycemic renal cells (Fig. 6).

However, in control cells, no such ultrastructural changes were observed in the morphology of ER. Tunicamycin was used as a positive control that induces ER stress by blocking the N-linked glycosylation of proteins during post-translational modifications. NRK 52E cells displayed noticeable ultrafine changes in ER morphology as indicated by enlargement of ER after 24 h treatment of tunicamycin demonstrating the ER stress conditions (Fig. 6). Naringenin treatment attenuated ER damage by preventing the ultrastructural changes in ER of hyperglycemic renal cells endorsing the protective effects of Naringenin during hyperglycemic nephrotoxicity.

**Fig. 6** Naringenin prevented ultrastructural changes in ER during hyperglycemic renal toxicity. Photomicrographs revealing the ultrafine changes in the morphology of ER in renal cells as visualized through TEM at original magnifications of 6500X, scale bar; 2  $\mu$ m, dimensions: 3622 $\times$ 2664 pixels and 30000X, scale bar; 0.5  $\mu$ m, dimensions: 3622 $\times$ 2664 pixels. Black arrows indicate the normal ER, Red arrows indicate the damaged or deformed ER structure in high glucose and tunicamycin treated renal cells. Yellow arrows indicate nearly normal ER upon Naringenin treatment in hyperglycemic renal cells



### Inhibition of ER stress averts metabolic aberrations and renal injuries in experimental diabetic rats

Hyperglycemia and hyperinsulinemia are the classical features of type 2 diabetes. Defective insulin signaling often leads to insulin resistance and dysregulation of glycemic control in insulin-sensitive tissues including kidneys (Schrauben et al. 2019). Therefore, to confirm hyperinsulinemic condition, insulin levels were measured in serum

samples of control, and STZ/nicotinamide treated diabetic rats through ELISA assay. Data suggests that insulin levels were significantly elevated (1.44 fold,  $p < 0.01$ ) in serum samples of experimental diabetic rats compared to control indicating the establishment of type 2 diabetes (Fig. 7A). However, supplementation of Naringenin significantly restored insulin level in diabetic rats demonstrating the insulin stabilizing potential of Naringenin. Further, the level of glucose in serum samples was measured to confirm the



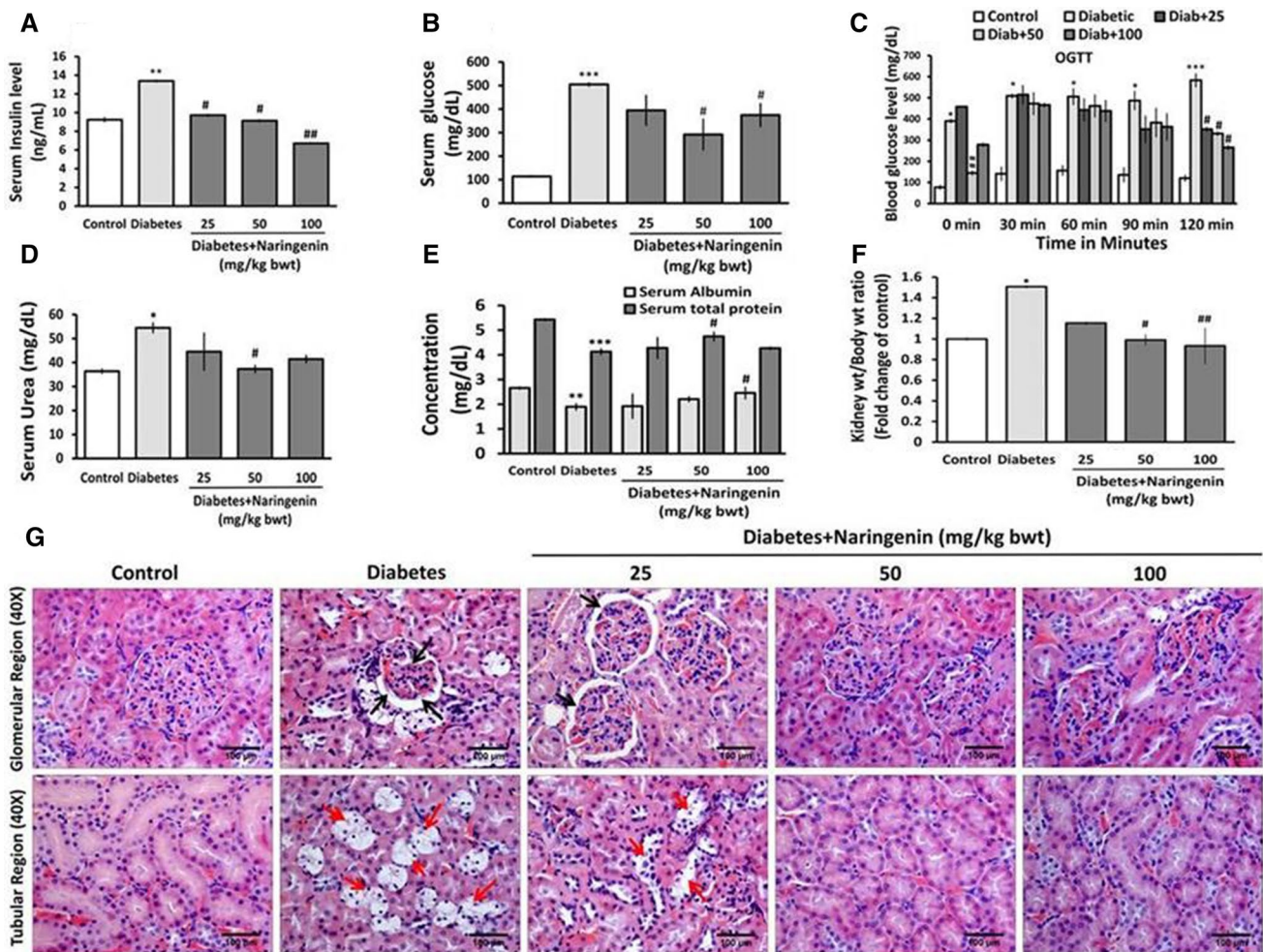


**Fig. 7** Naringenin attenuated hyperglycemia-induced metabolic perturbation and kidney damage in diabetic rats. **A** To confirm the establishment of type2 diabetic model, insulin levels were measured in rat serum. Bar graph represents the levels of serum insulin expressed in ng/mL of blood. **B** The bar graph shows the levels of glucose in rat serum after 4 weeks of diabetes induction and Naringenin supplementation. **C** Oral glucose tolerance test (OGTT) was conducted on control and treated animals. The bar graph represents the blood glucose levels at various time intervals. **D** Serum urea levels (mg/dL). **E** Serum albumin and serum total proteins (mg/dL). **F** The bar graph

shows kidney weight/body weight ratio expressed in fold change of control. **G** Histopathological lesions in the kidneys of control and treated rats were observed through H&E staining (magnification: renal tubules; 40X with scale bar 100  $\mu$ m and glomeruli; 40X with scale bar 100  $\mu$ m). Black arrows indicate the increased bowman's space and shrinkage of glomeruli red arrows indicate the tubular degeneration and loss of brush border cells. Data are presented as mean  $\pm$  SE. \*  $p < 0.05$ , \*\*  $p < 0.01$ , \*\*\*  $p < 0.001$  vs control and #  $p < 0.05$ , ##  $p < 0.01$  vs diabetic rats

stable hyperglycemic conditions. STZ/nicotinamide induced diabetic rats showed upsurged glucose levels (504 mg/dL) in their serum samples confirming the establishment of hyperglycemia. Diabetic rats treated with Naringenin (50 mg/kg bwt) reduced the serum glucose levels upto (291 mg/dL), affirming the anti-hyperglycemic property of Naringenin (Fig. 7B). The lower dose of Naringenin (25 mg/kg bwt), failed to decrease the serum glucose levels in diabetic rats (Fig. 7B). To further confirm the anti-hyperglycemic potential of Naringenin, an oral glucose tolerance test was performed. Diabetic rats showed poor glycaemic control as the blood glucose levels were constantly higher throughout

120 min, indicating impairment of insulin sensitization signals (Fig. 7C). Naringenin supplementation efficiently cleared the circulating blood glucose after 120 min compared to experimental diabetic rats confirming the anti-hyperglycemic potency of Naringenin (Fig. 7C). STZ/nicotinamide treatment causes stable hyperglycemia which further leads to impaired renal function. Further, Diabetic rats demonstrated a significant increase in serum urea levels (1.49 fold,  $p < 0.05$ ) compared to control while Naringenin treatment (50 mg/kg bwt) reduced the level of urea (0.68 fold,  $p < 0.05$ ) compared to diabetic rats (Fig. 7D). Serum albumin and serum total protein levels were also found

to decline in diabetic rats compared to control implicating hyperglycemia-induced renal dysfunction (Fig. 7E). A significant increase in the kidney weight/body weight ratio (1.5 fold,  $p < 0.05$ ) was observed in diabetic rats implicating hyperglycemia-induced kidney hypertrophy (Fig. 7F). Notably, diabetic rats treated with Naringenin attenuated abnormal change in kidney weight/body weight ratio advocating its reno-protective effects during diabetic renal toxicity (Fig. 7F).

Chronic hyperglycemia has been shown to cause structural changes in the kidneys during diabetes. Histopathological examination of kidneys showed noticeable changes in kidney architecture. H&E stained kidney sections demonstrated severe pathological changes in STZ/nicotinamide treated diabetic kidneys such as shrinkage of glomeruli, increased Bowman's capsular space, degeneration of tubular cells with severely engorged interstitial blood vessels and loss of brush border cells compared to control, confirming the occurrence of diabetic renal injuries. Interestingly, rats treated with Naringenin (50 and 100 mg/kg bwt) for 4 weeks prevented the shrinkage of glomeruli, tubular dilatation, loss of brush border cells and tubular degeneration compared to diabetic rats evidencing its renoprotective effects in experimental diabetic kidneys of STZ/nicotinamide induced diabetic rats (Fig. 7G). However, 25 mg/kg bwt dose of Naringenin could not avert the histopathological changes in diabetic kidneys. Therefore, the data suggest that 50 and 100 mg/kg bwt dose of Naringenin worked better than the low dose, i.e. 25 mg/kg bwt in abrogating renal injuries during hyperglycemic nephrotoxicity.

### Naringenin prevents hyperglycemia-induced apoptosis in vitro and in vivo

In this study so far, it was observed that hyperglycemia upregulated ER stress marker proteins in NRK 52E cells and STZ/nicotinamide induced diabetic kidney tissues, which were attenuated by Naringenin. Persistent activation of CHOP has been earlier reported by our group to induce apoptotic signaling cascade via inhibition of Bcl2 during diabetes (Pandey et al. 2019). Therefore, to confirm this, we measured the protein levels of anti-apoptotic marker Bcl2 and proapoptotic markers, including Bax and cleaved caspase 3. Further, immunoblotting studies revealed a significant increase in Bax/Bcl2 ratio (2.88 fold,  $p < 0.001$ ) after 24 h of tunicamycin treatment in NRK 52E cells compared to untreated cells confirming ER stress-induced proteotoxic apoptotic death (Fig. 8A). Interestingly, in hyperglycemic renal cells, Bax/Bcl2 ratio was significantly upregulated (3.96 fold,  $p < 0.001$ ) compared to control endorsing the activation of apoptotic signals during hyperglycemic renal toxicity. Conversely, Naringenin treatment prevented cell death as the Bax/Bcl2 ratio was significantly reduced (2.02

fold,  $p < 0.001$ ) compared to hyperglycemic renal cells (Fig. 8A). Cleavage of caspase 3 is a critical event in apoptosis. Hence, we examined the level of cleaved caspase 3 in tunicamycin and high glucose exposed renal cells. Western blot analysis revealed a significant increase in cleaved caspase 3 levels in tunicamycin (1.73 fold,  $p < 0.001$ ) and high glucose (1.47 fold,  $p < 0.001$ ) treated renal cells compared to control (Fig. 8B). Naringenin prevented cell death by arresting caspase 3 activation in hyperglycemic NRK 52E cells indicating its anti-apoptotic potential during hyperglycemic renal toxicity. To further confirm the anti-apoptotic effects of Naringenin, we assessed the ultrastructural changes in the cellular morphology of NRK 52E cells through TEM. Photomicrographs of tunicamycin treated renal cells revealed the ultrafine changes, including loss of cell architecture, damage and blebbing of the cell membrane and formation of apoptotic bodies indicating ER stress-induced apoptotic cell death (Fig. 8C). Similar changes were observed in high glucose treated renal cells indicating the loss of tubular cells through apoptotic death under hyperglycemic environment. Interestingly, co-treatment of Naringenin in hyperglycemic renal cells for 48 h prevented the loss of renal cells by inhibiting apoptotic cell death confirming its anti-apoptotic properties (Fig. 8C). Furthermore, activation of apoptosis was confirmed in kidney tissue lysates of STZ/nicotinamide treated diabetic rats. The ratio of Bax/Bcl2 and cleaved caspase 3 protein levels were measured through western blotting. Data revealed a significant upregulation in the Bax/Bcl2 ratio (2.68 fold,  $p < 0.001$ ) and cleaved caspase 3 (2.33 fold,  $p < 0.001$ ) indicating the activation of the apoptotic cascade in diabetic kidney tissues (Fig. 8D). Naringenin treatment maintained the ratio of pro- and anti-apoptotic proteins as evident by reduced Bax/Bcl2 ratio and concomitant blocking of the cleavage and activation of caspase 3 affirming its reno-protective capacity during hyperglycemic renal toxicity.

## Discussion

Diabetic nephropathy is one of the major pathological outcomes of chronic kidney disease leading to end-stage kidney failure globally. The molecular mechanisms underlying the physiopathology of the disease are highly complex and still being explored. However, many studies have demonstrated that oxidative stress (Mathur et al. 2018) and ER stress (Mo et al. 2019) may be the major pathogenic mechanisms contributing to the pathogenesis of DN. Interestingly, ER stress inhibition has been shown to give promising results to manage diabetic nephropathy (Cao et al. 2016). Preventive management of diabetic complications through different flavonoids, including Naringenin, is well known. Though, the unique mechanism, i.e. ER stress signaling and



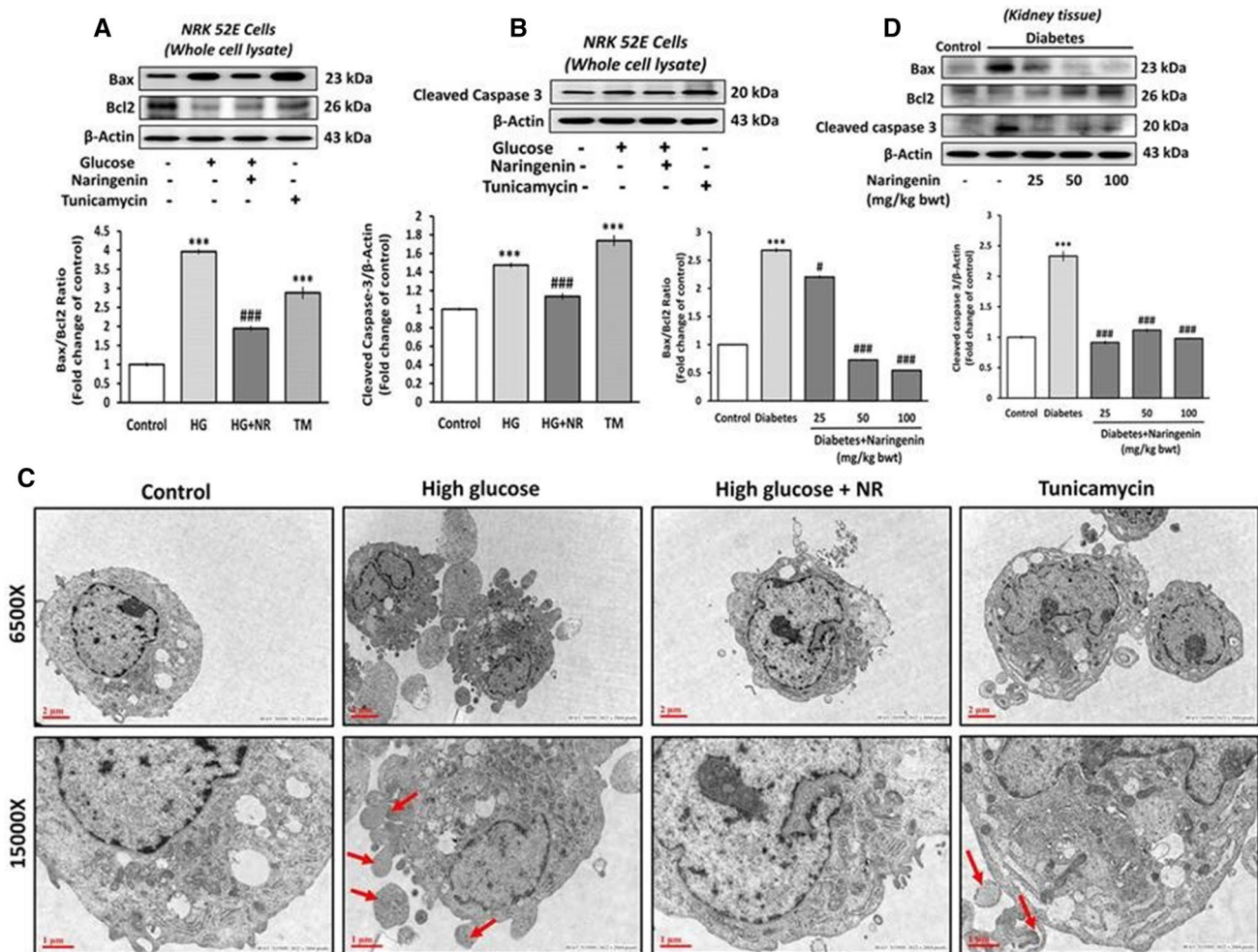


**Fig. 8** Naringenin inhibited hyperglycemia-induced apoptotic death in vitro and in vivo. Renal cells were co-treated with high glucose and Naringenin for 48 h. Tunicamycin (2  $\mu$ g/mL; 24 h) was used to induce ER stress in NRK 52E cells **A** Changes in Bax and Bcl2 protein levels were detected in cells/tissue lysates through western blot analysis. The bar graph shows the densitometric ratio of Bax and Bcl2 protein levels expressed in fold change of control. **B** Immunoblot of cleaved caspase 3 detected in NRK 52E cells. Bar graph indicates the cleaved caspase-3 protein expression in fold change of control. **C** Photomicrographs visualized under TEM with original

magnification 6500X; scale bar 2  $\mu$ m, dimensions: 3622 $\times$ 2664 pixels and 15000X; scale bar 1  $\mu$ m, dimensions: 3622 $\times$ 2664 pixels. Red arrows indicate the formation of apoptotic bodies in high glucose and tunicamycin treated cells. **D** Immunoblots of Bax, Bcl2 and cleaved caspase 3 were examined in kidney tissue lysates. The bar graph represents the densitometry of the Bax/Bcl2 ratio and cleaved caspase 3 proteins expressed in fold change of control.  $\beta$ -actin served as a loading control. Data are presented as mean  $\pm$  SD. \*\*\*  $p < 0.001$  vs control and #  $p < 0.05$ , ###  $p < 0.001$  vs HG/diabetes

its amelioration by Naringenin during diabetic renal toxicity is not been reported till the date.

In the present study, we have demonstrated the novel role of Naringenin in attenuating ER stress-induced renal cell death in hyperglycemic NRK 52E cells, and streptozotocin/nicotinamide induced diabetic Wistar rats. Previous reports from our lab as well as others have shown that Naringenin plays an important role in modulating apoptotic death in different cell types such as primary rat hepatocytes (Kapoor et al. 2013) and myocardial (H9c2) cells (Tang et al. 2017). However, its role in regulating hyperglycemia-induced ER stress in the renal system is not documented so far. In an

earlier study, Naringenin was found to be non-cytotoxic up to the concentration of 100  $\mu$ M in pancreatic  $\beta$ -cells (MIN6 cells). Although, at 200  $\mu$ M dose, Naringenin exerted its cytotoxic effects and decreased the viability of MIN6 cells up to 65% after 24 h of treatment (Rajappa et al. 2019). There are no studies, demonstrating the cytotoxic effects of Naringenin on NRK 52E cells. Therefore, we examined the toxicity pattern of Naringenin on NRK 52E cells to select a non-cytotoxic and effective dose for in vitro experiments. In our study, it was observed that Naringenin was non-cytotoxic to NRK 52E cells up to the highest concentration, i.e. 50  $\mu$ M. However, beyond this dose, Naringenin caused significant

cell death as evident by reduced viability of NRK 5E cells after 24, 48 and 72 h of treatment (Supl.Fig. 1b-d). Naringenin is reported to protect hypoxia/reoxygenation induced apoptosis in cardiomyocytes (H9c2 cells) at 80 and 160  $\mu\text{M}$  concentrations (Tang et al. 2017) and streptozotocin induced cytotoxicity in pancreatic beta cells (MIN6 cells) at 100  $\mu\text{M}$  dose (Rajappa et al. 2019). Results of co-treatment in this study showed that Naringenin (25 and 50  $\mu\text{M}$ ) prevented cell death in high glucose treated NRK 52E cells as evident through MTT, Alamar blue, propidium iodide uptake and Hoechst 33,258 staining (Fig. 1A-D) respectively. Therefore, we selected 25  $\mu\text{M}$  dose of Naringenin to examine its anti-ER stress and anti-oxidant potential during hyperglycemic renal toxicity.

Rising evidence suggests that prolonged hyperglycemic environment causes overproduction of ROS, which leads to oxidation of cellular macromolecules such as proteins owing to ER dysfunction and compromised anti-oxidant defense system (Pandey et al. 2019). The present study shows that Naringenin abrogates ROS generation in high glucose treated NRK 52E cells and streptozotocin/nicotinamide induced diabetic kidney tissues asserting its anti-oxidative capacity (Fig. 2A-B, Supl. Fig. 2a). Although, mitochondria are the major source of ROS generation, but other than mitochondria, ER is also involved in oxidative stress-mediated hyperglycemic renal toxicity. In this study, we found that treatment of tunicamycin, an ER stress inducer, significantly increased the ROS generation leading towards oxidative misfolding of polypeptides in ER, which further hampers proteo-homeostasis in ER (Fig. 2A-B). Excessive ROS generation during hyperglycemic stress can damage mitochondrial membrane lipids and reduces membrane potential, resulting in the initiation of the apoptotic cascade. Our data demonstrated that Naringenin prevented the loss of mitochondrial membrane potential in high glucose treated NRK 52E cells confirming its renoprotective potential (Fig. 2C). Overproduction of ROS has been linked with the declined anti-oxidant defense system in the pathogenesis of hyperglycemic renal toxicity (Chen et al., 2018). In our study, Naringenin treatment improved the anti-oxidant defense systems in hyperglycemic NRK 52E cells (Fig. 2D-F) and kidney tissues of STZ/nicotinamide treated experimental diabetic rats (Supl.Fig. 2b-d) evidencing the anti-oxidant potential of Naringenin.

Several studies have been reported so far, which demonstrate the involvement of ER stress in the progression and pathogenesis of diabetic kidney disease. Disruption in oxido-reductive balance has been found as a prevalent cause of ER dysfunction. Many chemical inhibitors of ER stress, including tauroursodeoxycholic acid (TUDCA), are reported to prevent renal tubular injuries through abrogating ER stress in the kidney tissues of db/db mice (Zhang et al. 2016). Phytochemicals are known to cause fewer adverse

effects and have emerged as an alternative strategy to manage diabetic kidney disease. Naringenin is reported to attenuate ER stress-induced apoptosis in cardiomyocytes (H9c2 cells) during hypoxia/reoxygenation (Tang et al. 2017). Activation of PERK/eIF2 $\alpha$  signaling pathway is shown to be a major contributor to the pathogenesis of several diseases, including in hyperglycemia-induced disorders (Pandey et al. 2019). Several pathological conditions like hyperglycemia cause aberrant activation of PERK pathway, which plays a cardinal role in the progression and pathophysiology of hyperglycemic nephrotoxicity (Tian et al. 2018). In this study increased, phosphorylation of PERK was observed, which was prevented by Naringenin treatment in vitro and in vivo indicating its ER stress regulatory effects (Fig. 3A, 4A). PERK-mediated phosphorylation of eIF2 $\alpha$  (an indicator of ER stress) inhibits the assembly of 80S ribosome and consequently, protein synthesis to reduce the protein load in already saturated ER (Rozpedek et al. 2016; Pandey et al. 2019). Our results show that Naringenin treatment prevents the phosphorylation of eIF2 $\alpha$  in hyperglycemic NRK 52E cells, and in the kidney tissues of STZ/nicotinamide treated diabetic Wistar rats (Figs. 3B, 4B). Tunicamycin was used to induce ER stress in NRK 52E cells, which served as a positive control of ER stress. Treatment of tunicamycin increased the levels of p-PERK and p-eIF2 $\alpha$  indicating the activation of ER stress in renal tubular cells (Fig. 3A-B). Under ER stress, IRE1 $\alpha$  gets phosphorylated, thereby activating its ribonuclease activity and initiates the splicing of mRNA encoding XBP1s protein. Immunoblotting and immunocytochemical studies showed that treatment of Naringenin suppressed the protein levels of XBP1s in hyperglycemic NRK 52E cells (Fig. 3C-E). Prolonged or severe ER stress often leads to the activation of proteotoxic apoptosis through multiple pathways. Phosphorylation of eIF2 $\alpha$  not only constrains the protein synthesis but also induces the expression of specific transcription factors, including ATF4 and CHOP. Generally, ATF4 regulates a wide array of genes, which play an important role in protein homeostasis and adaptation to cellular stress. However, under long-term ER stress conditions, ATF4 may also induce the activation of amino acid response elements (AARE) owing to the activation and expression of CHOP. Increased expression of ATF4 and CHOP is an important sign of chronic ER stress, which plays a pivotal role in inducing ER stress-mediated apoptotic cell death.

In this study, we found that high glucose treated NRK 52E cells, and STZ/nicotinamide induced experimental DN rats had a significant increment in the expression level of proteotoxic apoptotic marker proteins, including ATF4 and CHOP proteins (Fig. 3F-H and 4C-D). An important finding was that Naringenin downregulated the expression ATF4 and CHOP in hyperglycemic NRK 52E cells, and in the kidney tissues of STZ/nicotinamide induced experimental diabetic

rats (Fig. 3F-H and 4C-D). Furthermore, it has been shown that overexpression of CHOP accelerates apoptosis while CHOP deficient mice were protected from ER stress-induced apoptotic death under diabetic conditions (Oyadomari et al. 2002). Under ER stress conditions, ATF4 and CHOP translocate to the nuclear compartment and form a transcriptional complex with a 9 base pair sequence that regulates ER stress-related genes (Oyadomari and Mori 2004). In our study, we found that nuclear colocalization of ATF4 and CHOP was increased in high glucose, and tunicamycin treated NRK 52E cells (Fig. 5A). Further, ATF4 and CHOP were found to be increased in the nuclear fractions of diabetic kidney tissues confirming their nuclear translocation under diabetic conditions (Fig. 5B). Additionally, the interaction of ATF4 and CHOP was also increased in the nuclear compartment of diabetic kidney tissues as examined through co-immunoprecipitation studies (Fig. 5D). However, treatment of Naringenin prevented nuclear translocation of ATF4 and CHOP in vitro and in vivo (Fig. 5A-D). Hence, it can be conceived that the protective effects of Naringenin are associated with the inhibition of ER stress. Upregulation of CHOP is known to downregulate Bcl2 expression resulting into increased ratio of Bax/Bcl2 proteins culminating in programmed cell death (Li et al. 2015). Further, the effect of Naringenin on the expression of anti-apoptotic and apoptotic marker proteins was investigated. It was observed that Naringenin treatment prevented apoptosis by downregulation of Bax/Bcl2 ratio and cleavage and activation of caspase 3 in hyperglycemic NRK 52E cells and in the kidneys of experimental diabetic Wistar rats (Fig. 8A, 8B, 8D). Additionally, hyperglycemic renal cells displayed ultrastructural changes in ER such as the disintegration of the ER membrane and dilatation of ER sacs as observed in TEM micrographs (Fig. 6). Naringenin treatment not only reduced ER stress but also prevented the ultrafine changes in the morphology of ER in hyperglycemic renal cells advocating its anti-ER stress activity (Fig. 6). Furthermore, TEM micrographs showed membrane blebbing and formation of apoptotic bodies in presence of high glucose and tunicamycin confirming ER stress-induced apoptotic cell death (Fig. 8C). Naringenin not only reduced apoptotic marker proteins but also prevented the formation of apoptotic bodies proving its anti-apoptotic potential (Fig. 8C). Overall, the findings of the study suggest that the protective mechanism of Naringenin is associated with the suppression of ER stress.

## Conclusions

In conclusion, the current study demonstrates ER stress inhibitory capacity of Naringenin in hyperglycemic renal cells and STZ/nicotinamide induced diabetic rats. Naringenin treatment downregulated the expression of ER stress marker proteins, including p-PERK, p-eIF2 $\alpha$ , XBP1s, ATF4

and CHOP in vitro and in vivo. Supplementation of Naringenin reduced the nuclear translocation of proteotoxic apoptotic marker proteins, including ATF4 and CHOP in hyperglycemic NRK 52E cells and kidney tissues of experimental diabetic rats. Naringenin also averted ultrastructural changes in ER, prevented tubular cell apoptosis and kidney injuries during hyperglycemic nephrotoxicity affirming its protective capacity. Thus, the findings suggest that Naringenin can be exploited as a bioactive flavonoid in the management of hyperglycemic renal toxicity.

**Supplementary Information** The online version contains supplementary material available at <https://doi.org/10.1007/s12079-021-00644-0>.

**Acknowledgements** The authors are grateful to the Manuscript Review Committee of CSIR-Indian Institute of Toxicology Research for reviewing and providing the communication number (3694) to the manuscript. The authors are thankful to Dr. Beena Vamadevan and Mr. Pankaj Jagdale for their support in histopathology. We are grateful to Mr. Jai Shankar for his support in transmission electron microscopy.

**Author contributions** M.F.K., P.K., A.M., and V.K.P. conceived the idea to the project. M.F.K., A.M., and V.K.P. designed and performed the experiments and analyzed the data. M.F.K. wrote the original draft of the manuscript. P.K. provided the materials and reviewed the manuscript. M.F.K., A.M., V.K.P., and P.K. wrote and edited the manuscript. The final version of the manuscript was read and approved by all the authors.

**Funding** This work was supported by the Council of Scientific and Industrial Research (CSIR) project (Grant No.HCP0019) to PK. MFK and AM is thankful to the Council of Scientific and Industrial Research (CSIR) for providing Senior Research Fellowship (SRF) and VKP is thankful to University Grant Commission (UGC) for Senior Research Fellowship (SRF).

## Declarations

**Conflict of interest** The authors declare no conflict of interest regarding authorship and publication of this research article.

## References

- Acosta-Alvear D, Karagöz GE, Fröhlich F, Li H, Walther TC, Walter P (2018) The unfolded protein response and endoplasmic reticulum protein targeting machineries converge on the stress sensor IRE1. *eLife* 7:43036
- Almanza A, Carlesso A, Chintla C, Creedican S, Doultinos D, Leuzzi B, Luís A, McCarthy N, Montibeller L, More S, Papaioannou A, Püschel F, Sassano ML, Skoko J, Agostinis P, de Bellerocche J, Eriksson LA, Fulda S, Gorman AM, Healy S, Samali A (2019) Endoplasmic reticulum stress signalling - from basic mechanisms to clinical applications. *FEBS J* 286:241–278. <https://doi.org/10.1111/febs.14608>
- Burgos-Morón E, Abad-Jiménez Z, Marañón AM, Iannantuoni F, Escribano-López I, López-Domènech S, Salom C, Jover A, Mora V, Roldan I, Solá E, Rocha M, Víctor VM (2019) Relationship between oxidative stress, ER stress, and inflammation



- in Type 2 diabetes: the battle continues. *J Clin Med* 8:1385. <https://doi.org/10.3390/jcm8091385>
- Cao AL, Wang L, Chen X, Wang YM, Guo HJ, Chu S, Liu C, Zhang XM, Peng W (2016) Ursodeoxycholic acid and 4-phenylbutyrate prevent endoplasmic reticulum stress-induced podocyte apoptosis in diabetic nephropathy. *Lab Investigation* 96:610–622. <https://doi.org/10.1038/labinvest.2016.44>
- Chen X, Fang M (2018) Oxidative stress mediated mitochondrial damage plays roles in pathogenesis of diabetic nephropathy rat. *Eur Rev Med Pharmacol Sci* 22:5248–5254. [https://doi.org/10.26355/eurrev\\_201808\\_15723](https://doi.org/10.26355/eurrev_201808_15723)
- Cossarizza A, Baccarani-Contri M, Kalashnikova G, Franceschi C (1993) A new method for the cytofluorimetric analysis of mitochondrial membrane potential using the J-aggregate forming lipophilic cation 5,5',6,6'-tetrachloro-1,1',3,3'-tetraethylbenzimidazolcarbocyanine iodide (JC-1). *Biochem Biophys Res Commun* 197(40):45. <https://doi.org/10.1006/bbrc.1993.2438>
- Cottrell GS, Padilla B, Pikios S, Roosterman D, Steinhoff M, Gehringer D, Grady EF, Bunnett NW (2006) Ubiquitin-dependent down-regulation of the neurokinin-1 receptor. *J Biol Chem* 281(38):27773–27783. <https://doi.org/10.1074/jbc.M603369200>
- Ghemrawi R, Battaglia-Hsu SF, Arnold C (2018) Endoplasmic reticulum stress in metabolic disorders. *Cells* 7:63. <https://doi.org/10.3390/cells7060063>
- Ghezzi AC, Cambri LT, Botezelli JD, Ribeiro C, Dalia RA, de Mello MA (2012) Metabolic syndrome markers in wistar rats of different ages. *Diabetol Metab Syndr* 4:16. <https://doi.org/10.1186/1758-5996-4-16>
- Gotoh T, Oyadomari S, Mori K, Mori M (2002) Nitric oxide-induced apoptosis in RAW 264.7 macrophages is mediated by endoplasmic reticulum stress pathway involving ATF6 and CHOP. *J Biol Chem* 277(14):12343–12350. <https://doi.org/10.1074/jbc.M107988200>
- Gurley SB, Ghosh S, Johnson SA, Azushima K, Sakban RB, George SE, Maeda M, Meyer TW, Coffman TM (2018) Inflammation and immunity pathways regulate genetic susceptibility to diabetic nephropathy. *Diabetes* 67:2096–2106. <https://doi.org/10.2337/db17-1323>
- Ju Y, Su Y, Chen Q, Ma K, Ji T, Wang Z, Li W, Li W (2019) Protective effects of Astragaloside IV on endoplasmic reticulum stress-induced renal tubular epithelial cells apoptosis in type 2 diabetic nephropathy rats. *Biomed Pharmacother* 109:84–92. <https://doi.org/10.1016/j.biopha.2018.10.041>
- Kapoor R, Kakkar P (2014) Naringenin accords hepatoprotection from streptozotocin induced diabetes in vivo by modulating mitochondrial dysfunction and apoptotic signaling cascade. *Toxicol Rep* 1:569–581. <https://doi.org/10.1016/j.toxrep.2014.08.002>
- Kapoor R, Srivastava S, Kakkar P (2009) Bacopa monnieri modulates antioxidant responses in brain and kidney of diabetic rats. *Environ Toxicol Pharmacol* 27:62–69. <https://doi.org/10.1016/j.etap.2008.08.007>
- Kapoor R, Rizvi F, Kakkar P (2013) Naringenin prevents high glucose-induced mitochondria-mediated apoptosis involving AIF, EndoG and caspases. *Apoptosis* 18:9–27. <https://doi.org/10.1007/s10495-012-0781-7>
- Larson EM, Doughman DJ, Gregerson DS, Obritsch WF (1997) A new, simple, nonradioactive, nontoxic in vitro assay to monitor corneal endothelial cell viability. *Invest Ophthalmol vis Sci* 38:1929–1933
- Li Y, Guo Y, Tang J, Jiang J, Chen Z (2015) New insights into the roles of CHOP-induced apoptosis in ER stress. *Acta Biochimica Biophysica Sinica* 47:146–147. <https://doi.org/10.1093/abbs/gmu128>
- Liu X, Green RM (2019) Endoplasmic reticulum stress and liver diseases. *Liver Res* 3:55–64. <https://doi.org/10.1016/j.livres.2019.01.002>
- Liu G, Sun Y, Li Z, Song T, Wang H, Zhang Y, Ge Z (2008) Apoptosis induced by endoplasmic reticulum stress involved in diabetic kidney disease. *Biochem Biophys Res Commun* 370:651–656. <https://doi.org/10.1016/j.bbrc.2008.04.031>
- Masiello P, Broca C, Gross R, Roye M, Manteghetti M, Hillaire-Buys D, Novelli M, Ribes G (1998) Experimental NIDDM: development of a new model in adult rats administered streptozotocin and nicotinamide. *Diabetes* 47:224–229. <https://doi.org/10.2337/diab.47.2.224>
- Mathur A, Pandey VK, Kakkar P (2018) Activation of GSK3 $\beta$ /TrCP axis via PHLPP1 exacerbates Nrf2 degradation leading to impairment in cell survival pathway during diabetic nephropathy. *Free Radical Biol Med* 120:414–424. <https://doi.org/10.1016/j.freeradbiomed.2018.04.550>
- Mo JS, Choi D, Han YR, Kim N, Jeong HS (2019) Morin has protective potential against ER stress induced apoptosis in renal proximal tubular HK-2 cells. *Biomed Pharmacother* 112:108659. <https://doi.org/10.1016/j.biopha.2019.108659>
- Mosmann T (1983) Rapid colorimetric assay for cellular growth and survival: application to proliferation and cytotoxicity assays. *J Immunol Methods* 65:55–63. [https://doi.org/10.1016/0022-1759\(83\)90303-4](https://doi.org/10.1016/0022-1759(83)90303-4)
- Oyadomari S, Mori M (2004) Roles of CHOP/GADD153 in endoplasmic reticulum stress. *Cell Death Differ* 11(4):381–389. <https://doi.org/10.1038/sj.cdd.4401373>
- Oyadomari S, Koizumi A, Takeda K, Gotoh T, Akira S, Araki E, Mori M (2002) Targeted disruption of the chop gene delays endoplasmic reticulum stress-mediated diabetes. *J Clin Invest* 109(4):525–532. <https://doi.org/10.1172/JCI14550>
- Pandey VK, Mathur A, Khan MF, Kakkar P (2019) Activation of PERK-eIF2 $\alpha$ -ATF4 pathway contributes to diabetic hepatotoxicity: attenuation of ER stress by Morin. *Cell Signal* 59:41–52. <https://doi.org/10.1016/j.cellsig.2019.03.008>
- Pobres K, Poet GJ, Hendershot LM (2019) The endoplasmic reticulum (ER) chaperone BiP is a master regulator of ER functions: getting by with a little help from ERdj friends. *J Biol Chem* 294:2098–2108. <https://doi.org/10.1074/jbc.REV118.002804>
- Rajappa R, Sireesh D, Salai MB, Ramkumar KM, Sarvajayakesavalu S, Madhunapantula SV (2019) Treatment with naringenin elevates the activity of transcription factor Nrf2 to protect pancreatic  $\beta$ -Cells from streptozotocin-induced diabetes in vitro and in vivo. *Front Pharmacol* 9:1562. <https://doi.org/10.3389/fphar.2018.01562>
- Rozpedek W, Pytel D, Mucha B, Leszczynska H, Diehl JA, Majsterek I (2016) The Role of the PERK/eIF2 $\alpha$ /ATF4/CHOP signaling pathway in tumor progression during endoplasmic reticulum stress. *Curr Mol Med* 16:533–544. <https://doi.org/10.2174/1566524016666160523143937>
- Saxena S, Mathur A, Kakkar P (2019) Critical role of mitochondrial dysfunction and impaired mitophagy in diabetic nephropathy. *J Cell Physiol* 234:19223–19236. <https://doi.org/10.1002/jcp.28712>
- Schrauben SJ, Jepson C, Hsu JY, Wilson FP, Zhang X, Lash JP, Robinson BM, Townsend RR, Chen J, Fogelfeld L, Kao P, Landis JR, Rader DJ, Hamm LL, Anderson AH, Feldman HI (2019) Insulin resistance and chronic kidney disease progression, cardiovascular events, and death: findings from the chronic renal insufficiency cohort study. *BMC Nephrol* 20:60. <https://doi.org/10.1186/s12882-019-1220-6>
- Shukla S, Rizvi F, Raisuddin S, Kakkar P (2014) FoxO proteins' nuclear retention and BH3-only protein Bim induction evoke mitochondrial dysfunction-mediated apoptosis in berberine-treated HepG2 cells. *Free Radical Biol Med* 76:185–199. <https://doi.org/10.1016/j.freeradbiomed.2014.07.039>
- Smith PK, Krohn RI, Hermanson GT, Mallia AK, Gartner FH, Provenzano MD, Fujimoto EK, Goetze NM, Olson BJ, Klenk DC (1985)



- Measurement of protein using bicinchoninic acid. *Anal Biochem* 150:76–85. [https://doi.org/10.1016/0003-2697\(85\)90442-7](https://doi.org/10.1016/0003-2697(85)90442-7)
- Sulaiman MK (2019) Diabetic nephropathy: recent advances in pathophysiology and challenges in dietary management. *Diabetol Metab Syndr* 11:7. <https://doi.org/10.1186/s13098-019-0403-4>
- Sun XY, Qin HJ, Zhang Z, Xu Y, Yang XC, Zhao DM, Li XN, Sun LK (2016) Valproate attenuates diabetic nephropathy through inhibition of endoplasmic reticulum stress-induced apoptosis. *Mol Med Rep* 13:661–668. <https://doi.org/10.3892/mmr.2015.4580>
- Tang JY, Jin P, He Q, Lu LH, Ma JP, Gao WL, Bai HP, Yang J (2017) Naringenin ameliorates hypoxia/reoxygenation-induced endoplasmic reticulum stress-mediated apoptosis in H9c2 myocardial cells: involvement in ATF6, IRE1 $\alpha$  and PERK signaling activation. *Mol Cell Biochem* 424:111–122. <https://doi.org/10.1007/s11010-016-2848-1>
- Tian N, Gao Y, Wang X, Wu X, Zou D, Zhu Z, Han Z, Wang T, Shi Y (2018) Emodin mitigates podocytes apoptosis induced by endoplasmic reticulum stress through the inhibition of the PERK pathway in diabetic nephropathy. *Drug design Develop Therap* 12:2195–2211. <https://doi.org/10.2147/DDDT.S167405>
- Tsuchiya Y, Saito M, Kadokura H, Miyazaki JI, Tashiro F, Imagawa Y, Iwawaki T, Kohno K (2018) IRE1-XBP1 pathway regulates oxidative proinsulin folding in pancreatic  $\beta$  cells. *J Cell Biol* 217:1287–1301. <https://doi.org/10.1083/jcb.201707143>
- Van Krieken R, Mehta N, Wang T, Zheng M, Li R, Gao B, Ayaub E, Ask K, Paton JC, Paton AW, Austin RC, Krepinsky JC (2019) Cell surface expression of 78-kDa glucose-regulated protein (GRP78) mediates diabetic nephropathy. *J Biol Chem* 294:7755–7768. <https://doi.org/10.1074/jbc.RA118.006939>
- Zhang J, Fan Y, Zeng C, He L, Wang N (2016) tauroursodeoxycholic acid attenuates renal tubular injury in a mouse model of type 2 diabetes. *Nutrients* 8:589. <https://doi.org/10.3390/nu8100589>
- Zobeiri M, Belwal T, Parvizi F, Naseri R, Farzaei MH, Nabavi SF, Sureda A, Nabavi SM (2018) Naringenin and its Nano-formulations for Fatty Liver: cellular modes of action and clinical perspective. *Curr Pharm Biotechnol* 19:196–205. <https://doi.org/10.2174/1389201019666180514170122>

**Publisher's Note** Springer Nature remains neutral with regard to jurisdictional claims in published maps and institutional affiliations.